

Developing a Plastic Hinge Model for RC Beams Prone to Progressive Collapse

Farzad Rouhani

A Thesis

in

The Department

of

Building, Civil and Environmental Engineering

Presented in Partial Fulfillment of the Requirements

for the Degree of Master of Applied Science (Civil Engineering) at

Concordia University

Montreal, Quebec, Canada

November 2015

© Farzad Rouhani, 2015

CONCORDIA UNIVERSITY
School of Graduate Studies

This is to certify that the thesis prepared

By: Farzad Rouhani

Entitled: Developing a Plastic Hinge Model for RC Beams Prone to
Progressive Collapse

and submitted in partial fulfillment of the requirements for the degree of

Master of Applied Science (Civil Engineering)

complies with the regulations of the University and meets the accepted standards with respect to originality and quality.

Signed by the final examining committee:

_____ Lucia Tirca	Chair, Examiner
_____ Ramin Sedaghati	Examiner
_____ Ashutosh Bagchi	Examiner
_____ Lan Lin	Co-Supervisor
_____ Khaled Galal	Co-Supervisor

Approved by _____
Chair of Department or Graduate Program Director

November 2015 _____
Dean of Faculty

ABSTRACT

Developing a Plastic Hinge Model for RC beams prone to Progressive Collapse

Farzad Rouhani

The US General Service Administration (GSA) 2013 Guidelines specify the procedures and the minimum requirements for the design and evaluation of the new and existing buildings against progressive collapse due to an instantaneous removal of vertical load bearing elements (i.e., columns). The objective of this study is to assess the modeling parameters for reinforced concrete (RC) beams specified in the GSA 2013. Three types of RC buildings located in high, moderate and low seismic zones in Canada are designed according to the 2010 edition of the National Building Code of Canada. They were designed to have ductile, moderately ductile, and conventional seismic force resisting system (SFRS). In total, 27 three-dimensional finite element models are developed using ABAQUS by considering the design variables, such as span length, depth of the section, and the reinforcement ratio. Nonlinear pushdown analyses are conducted by increasing the vertical displacement at the location where the column is removed. The bending moment at the critical section of the beams is monitored throughout the analysis. Based on the analysis results, moment-rotation curve for beam for each type of the building is proposed. In addition, it is found out in the study that the detailing of the seismic design has significant effect on the progressive collapse resistance.

Acknowledgements

First and foremost, I would like to thank God, who has always been blessing and making me whom I am today. Also, I would like to thank many people who made this thesis possible.

I wish to express my sincere gratitude to my supervisors, Dr. Lan Lin and Dr. Khaled Galal, for their efforts and guidance during the course of this study. Throughout my thesis, they continuously supported me technically and financially and provided encouragement. I would have been lost without them.

There are no proper words to convey my deepest gratitude and respect to my lovely parents, Zahra Fatemi and Hossein Rouhani, for their unfailing emotional support. They were the emotional and moral source of support. This thesis would certainly not have existed without them. Therefore, I dedicated this thesis to them.

I am indebted to many of my friends for providing a stimulating environment for me to learn and grow. I especially acknowledge my friend Mr. Hamid Arabzadeh who helped me get through the difficult times, and for all of his technical supports.

Notations

a	Chord rotation of plastic hinge corresponding to the maximum bending moment capacity
d_c	Degradation of elastic stiffness in compression
d_t	Degradation of elastic stiffness in tension
e	Chord rotation of plastic hinge
E_c	Initial (undamaged) modulus of elasticity of concrete
f'_c	Specified compressive strength of concrete
f_t	Tensile strength
f_y	Yielding stress of reinforcing bars
f_u	Ultimate stress of reinforcing bars
h	Height of the concrete beam section
I_E	Importance factor
K_e	Elastic stiffness of the beam
M_V	Higher mode effect factor
Q_{UD}	Demand resulting from the analysis
Q_{CE}	Capacity of the member
R_d	Ductility-related force modification factor

R_o	Overstrength-related force modification factor
$S(T_a)$	Design spectral acceleration at the fundamental lateral period
T_a	Fundamental lateral period
V	Seismic base shear force
V_{min}	Minimum lateral earthquake shear force
V_{max}	Maximum lateral earthquake shear force
W	Total seismic weight
ε_c^{pl}	Equivalent plastic strains in compression
ε_c^{cr}	Cracking strain in compression
ε_t^{pl}	Equivalent plastic strains in tension
ε_t^{cr}	Cracking strain in tension
ε_{co}^{el}	Elastic strain in compression
ε_{to}^{el}	Elastic strain in tension
$\varepsilon_{50c(u)}$	Strain corresponding to the stress equal to 50% of the maximum strength of confined or un-confined concrete
ε_y	Yielding strain of reinforcing bars
ε_u	Ultimate strain of reinforcing bars
σ_{c0}	Initial yield in compression

σ_{cu}	Ultimate compression stress
σ_{t0}	Failure stress in tension
σ_t	Tensile stress
Δ	Displacement at the bottom of the removed column
η	$\frac{\rho - \rho'}{\rho_b}$
ρ	Ratio of tension reinforcement
ρ'	Ratio of compression reinforcement
ρ_b	Balanced reinforcement ratio

TABLE OF CONTENTS

LIST OF TABLES	x
LIST OF FIGURES	xi
Chapter 1: INTRODUCTION	1
1.1 Motivation	1
1.2 Objective of the study.....	3
1.3 Outline of the thesis.....	4
Chapter 2: LITERATURE REVIEW	6
2.1 Introduction	6
2.2 Previous studies on progressive collapse	10
2.3 Existing Guidelines	16
2.3.1 Overview of 2003 GSA	16
2.3.2 Overview of 2013 GSA	24
2.4 Progressive collapse analysis	27
2.5 Summary	30
Chapter 3: DESIGN OF RC MOMENT RESISTING FRAMES.....	31
3.1 Description of studied buildings.....	31
3.2 Design loads	33
3.2.1 Gravity loads.....	33
3.2.2 Seismic loads	33
3.3 Design of frames	37
3.4 Summary	38
Chapter 4: PROPOSED MODEL FOR RC BEAMS' PLASTIC HINGES.....	51
4.1 Introduction	51
4.2 Modelling techniques	52
4.2.1 Elements.....	52
4.2.2 Steel bars.....	53

4.2.3 Concrete	55
4.2.4 Cracking and failure of concrete.....	57
4.2.5 Interaction between concrete and steel bars.....	59
4.2.6 Meshing.....	59
4.3 Analysis results.....	63
4.3.1 Response curves.....	63
4.3.2 Development of parameters for modelling plastic hinges in beams.....	67
4.3.3 Prediction of the modelling parameters	70
4.3.4 Comparison with the parameters proposed in 2013 GSA.....	72
4.4 Summary	73
Chapter 5: CONCLUSIONS AND RECOMMENDATIONS	75
5.1 Introduction	75
5.2 Conclusions	76
5.3 Recommendations for future research.....	78
Appendix A: DESIGN OF REINFORCEMENT FOR BEAMS	79
A.1 Design of flexure reinforcement.....	79
A.1.1 Design singly reinforced sections	79
A.1.2 Design doubly reinforced sections.....	81
A.1.3 Minimum and maximum reinforcement	82
A.2 Design of shear reinforcement	82
A.3 Additional considerations for seismic design of beams	84
A.4 Sample of design	86
A.4.1 Flexure design.....	86
A.4.2 Shear design	87
A.4.3 Additional consideration for seismic design.....	88
REFERENCES.....	90

LIST OF TABLES

Table 2.1 Damage control and building performance levels	18
Table 3.1 Design gravity loads	33
Table 3.2 Design parameters for the frames	36
Table 3.3 Dimensions and the longitudinal and transverse reinforcement of beams in Toronto.....	39
Table 3.4 Dimensions and longitudinal and transverse reinforcement of beams in Montreal.....	40
Table 3.5 Dimensions and longitudinal and transverse reinforcement of beams in Vancouver	41
Table 4.1 Mean values for the modelling parameters proposed.	70

LIST OF FIGURES

Figure 2.1 Cases of collapsed and non-collapsed buildings due to impacts	9
Figure 2.2 Overall flow for consideration of progressive collapse adopted from GSA (2003)	21
Figure 2.3 Applicability flow chart adopted from GSA (2013).....	26
Figure 2.4 Definition of the actions adopted from GSA (2013) (a) Deformation-controlled actions, (b) Force-controlled actions	29
Figure 3.1 Plan of floors and elevation of longitudinal frames of the building (span = 6.0 m).....	32
Figure 3.2 Seismic design spectra for Toronto, Montreal, and Vancouver, site class C, 5% damping.	35
Figure 3.3 Distribution of the seismic force along the height of the building	36
Figure 3.4 Layout of the reinforcement of the beams in Toronto.....	42
Figure 3.5 Layout of the reinforcement of the beams in Montreal	45
Figure 3.6 Layout of the reinforcement of the beams in Vancouver	48
Figure 4.1 Critical frame with column removal.....	52
Figure 4.2 Schematic 3D ABAQUS model of the studied beam-column assembly.....	53
Figure 4.3 Stress-strain curve for the longitudinal and transverse steel bars.....	54
Figure 4.4 Stress-strain curve for concrete under compression and tension.....	56
Figure 4.5 Response of concrete to uniaxial loading: (a) tension, (b) compression adapted from ABAQUS	58
Figure 4.6 Cases for the sensitivity analysis on meshing	62
Figure 4.7 Beam responses from the sensitivity analyses.....	63

Figure 4.8 Beam response curves: (a) ductile beams, (b) moderately ductile beams, (c) conventional beam.....	65
Figure 4.9 Multi-linear backbone curve for modeling plastic hinges in beam (a) ductile and moderately ductile beams, (b) conventional beams.....	68
Figure 4.10 Comparison of the value for parameter a' based on the proposed model and 2013 GSA.....	72
Figure 4.11 Comparison of the proposed model with 2013 GSA criteria (a) ductile/moderately ductile beams, (b) conventional beams	74

Chapter 1

INTRODUCTION

1.1 Motivation

Since the partial collapse of the Ronan Point Apartment Building in London in 1968, design of building structures against progressive collapse have brought attention to researchers around the world. Furthermore, comprehensive research work has been conducted after the collapse of the World Trade Center Twin Towers in 2001. Progressive collapse can be initiated by a variety of abnormal conditions, such as impact (e.g., aircraft/vehicular collision), pressure loads (e.g., gas explosion) or overloading on the structure. These types of loads are mostly associated with the uncertainty in magnitude while the duration of impulse is significantly short, which might range from a few milliseconds up to 1-2 seconds. Although the occurrence rate of these events is relatively low, they might cause significant damage to structures and catastrophic losses.

According to the current building design codes, including the National Building Code of Canada (NBCC 2010) and the International Building Code (IBC 2015), the typical loads considered in the design of building structures are: dead, live, wind, and earthquake loads. Moreover, most of the existing buildings were not designed for the loads due to disproportionate collapse, and they might be vulnerable to progressive collapse under any of the conditions mentioned above.

U.S. General Service Administration (GSA) published guidelines for the progressive collapse resistance of buildings in 2003 and 2013, respectively. It should be noted that no guidelines on progressive collapse analysis are available in Canada. According to GSA, progressive collapse is defined as an event triggered by the local failure of the primary structural members due to the column removal, which might, in turn, cause the collapse of the adjacent members. The latest 2013 Guidelines were developed based on the seismic provisions of ASCE-41.13 (2014) by considering the structural integrity, ductility, and nonlinear behaviour due to the sudden removal of a column. Requirements for redundancy, overall structural integrity and resilience specified by the American Concrete Institution (ACI) were also considered in GSA Guidelines. In addition, United States Department of Defense (DoD) issued guidance on protection of facilities in case of abnormal loading and progressive collapse in 2001 and 2005, respectively.

Currently, GSA and DoD are the two commonly used guidelines for evaluating the progressive collapse resistance of building structures. The typical approach considered in GSA and DoD is designated as Alternative Path Method (APM). In APM, first, instantaneous loss of a vertical load-bearing element is assumed, i.e., a column is removed; then the capability of the beam elements supported by the column is evaluated. More specifically, the two major response parameters considered in APM are the vertical deflection and chord rotation of beams. It should be made clear that APM doesn't focus on the scenario that leads to the column removal itself. Therefore, this threat-independent method aims to provide redundancy to the structure in order to resist progressive collapse if it happens, i.e., the capability of beams and remaining columns is examined only after the column is removed.

In order to comply with the requirements of APM, several analysis procedures are specified in GSA and DoD, namely, linear static, nonlinear static, and nonlinear dynamic. The acceptance criteria for progressive collapse analysis are based on the response of beams; however, it is known that the capability of other elements (e.g., columns) also contributes to the overall resistance of the building against progressive collapse.

Although the results from the experimental tests and numerical analyses have made significant contribution to the latest GSA Guidelines published in 2013, there is still a lack of detailed implementation rules for the numerical modeling of progressive collapse analysis. In addition, by comparing the acceptance criteria in 2013 GSA with 2003 GSA, it has been found that the level of the new criteria is much higher than that of the old ones. Since the evaluation results of the building performance against progressive collapse depends very much on the acceptance criteria given in the Guidelines, they must be validated through experimental or numerical studies.

1.2 Objective of the study

The objective of this study is to investigate the performance of reinforced concrete frame buildings against progressive collapse. To achieve this objective, the following tasks were carried out in the study,

- (a) Design 27 four-storey reinforced concrete moment-resisting frame buildings located in Toronto, Montreal, and Vancouver that represent the low, moderate, and high seismic hazard zones in Canada, respectively.
- (b) Propose moment-rotation curves to simulate the nonlinear behaviour of plastic hinges due to column removal. Three-dimensional finite element analyses were

conducted on a beam-column assembly using the structural analysis software ABAQUS.

- (c) Compare the proposed curves with those specified in 2013 GSA.
- (d) Equations for prediction of the chord rotations corresponding to the maximum capacity and the first yielding of the beam were proposed.

1.3 Outline of the thesis

The material in this thesis is presented in 5 chapters and one appendix. Chapter 2 serves as literature review; Chapter 3 provides background material (i.e., design of the buildings) that is used in the research work presented in Chapter 4. The main conclusions from the research are given in Chapter 5.

Chapter 2 summarizes the previous studies on progressive collapse analysis. A comparison between the 2003 and 2013 GSA Guidelines is also presented in this chapter.

Chapter 3 describes the design of the buildings used in this study. Twenty seven 4-storey reinforced concrete moment resisting buildings assumed to be in Toronto, Montreal, and Vancouver were designed according to the 2010 edition of the National Building Code of Canada. More specifically, the span lengths considered are 4.0 m, 6.0 m, and 8.0 m. The reinforcement ratios are the minimum and maximum specified in the current Standard for design of concrete structures; and the one in between. The details of reinforcement of the designed buildings are presented in the Appendix A.

Chapter 4 presents the nonlinear finite element modeling of the beam-column assembly of the 27 buildings subjected to the column removal using the ABAQUS software. This chapter focuses on the techniques for modeling the beam-column elements

with the loss of one column below the beam, and the development of the moment-rotation curves to simulate the nonlinear behaviour of beams in the event. Finally, **Chapter 5** summarizes the main findings and conclusions from this study, and provides recommendations for future research.

Chapter 2

LITERATURE REVIEW

2.1 Introduction

The collapse of a part of the 22-storey **Ronan Point Apartment Building** in London, England in 1968 (Shankar 2004) is normally considered as the first example of the progressive collapse of building structures. The gas explosion at the 18th floor of the building triggered collapse of the corner slabs at the upper floors (above the 18th floor) that was followed by collapse of all corner slabs of the building (Fig. 2.1a). From a total of 260 residents, four were killed and seventeen were injured. The failure of the building was due mainly to the weakness of the joints connecting the walls to the floor slabs, which could not provide an alternative path to transfer the loads during the event (Pearson and Delatte 2005).

L'Ambiance Plaza Building was a 16-storey residential building in Bridgeport, Connecticut, the United States. On April 23, 1987, the partially erect frame completely collapsed during construction (Fig. 2.1b), which killed 28 workers on site. High stresses in concrete on the slabs developed during the erection of the frame was believed to be a major cause of the collapse (Heger 2006). This accident led to a nation-wide investigation on the safety of lifting slabs in construction as well as a temporary suspension on its use in the state of Connecticut (Dusenberry 2002).

A typical example of progressive collapse is the collapse of the **Alfred P. Murrah Federal Building** in Oklahoma City, due to a bomb explosion at the ground level in April 1995 (National Academy of Science 1995). A former soldier and security guard parked a truck in front of the building with the intention of committing mass murder. Three columns at the first storey were highly damaged, which caused the total collapse of almost half of the building (Fig. 2.1c). The building was demolished about a month after the event.

The collapse of the **Sampoong Department Store Building** (Fig. 2.1d) on June 29, 1995 was another example of the progressive collapse. The accident caused 502 deaths and injured 937 others, and was considered as the most significant disaster in the history of South Korea. The failure of the building was mainly attributed to overloading due to a change in the function of the building. More specifically, the fifth floor of the original building, which was supposed to house a skating rink, was remodelled to hold eight restaurants. In addition, it was found that the weight of the air conditioners installed on the roof increased the design dead load by about three times more than that specified in the code. Due to the overloading on the roof and the 5th floor, the columns failed first followed by the collapse of the south wing of the building.

With the increasing number of terrorist attacks, safety of government buildings has become a major concern after the collapse of the Twin Towers of the **World Trade Centre** on September 11, 2001. Two hijacked airplanes hit the north and south Towers within 15 minutes, which caused the collapse of the towers within two hours after the attack (Fig. 2.1e). Because of the redundancy of the tube-frame that was used as the main structural system, the Towers sustained the damage caused by the plane crashes, i.e., they did not collapse immediately. According to the study on the performance of the building published

by Federal Emergency Management Agency (FEMA 403), it was believed that fires triggered by the fuel of the jets weakened the connections of the steel trusses of the floor system, which led to the collapse of the towers.

As described above, a building could collapse or partially collapse due to a number of reasons, such as gas explosion, bomb attack, plane crash, etc. However, there are cases that the building survived, i.e., did not collapse, during the impact.

A building beside **Bankers Trust Building** collapsed in 1970 (Fig. 2.1f). The debris of the collapsed building hit the Bankers Trust Building, and caused severe damage to several columns. The zone of structural damage remained confined to one structural bay in the floors below. Therefore, progressive collapse was not triggered in the Bankers Trust Building given the extremely bad condition of the columns (Smilowitz et al. 2002).

The **Pentagon Building** in Washington D.C. was also attacked by a hijacked airplane on September 11, 2001. However, the building performed quite well during the event, and the progressive collapse that happened to the World Trade Center Twin Towers was not triggered in this case (Fig. 2.1g). After an intensive investigation, it was reported that sufficient structural redundancy was provided in the building for the progressive collapse resistance (Mlaker et al. 2003).

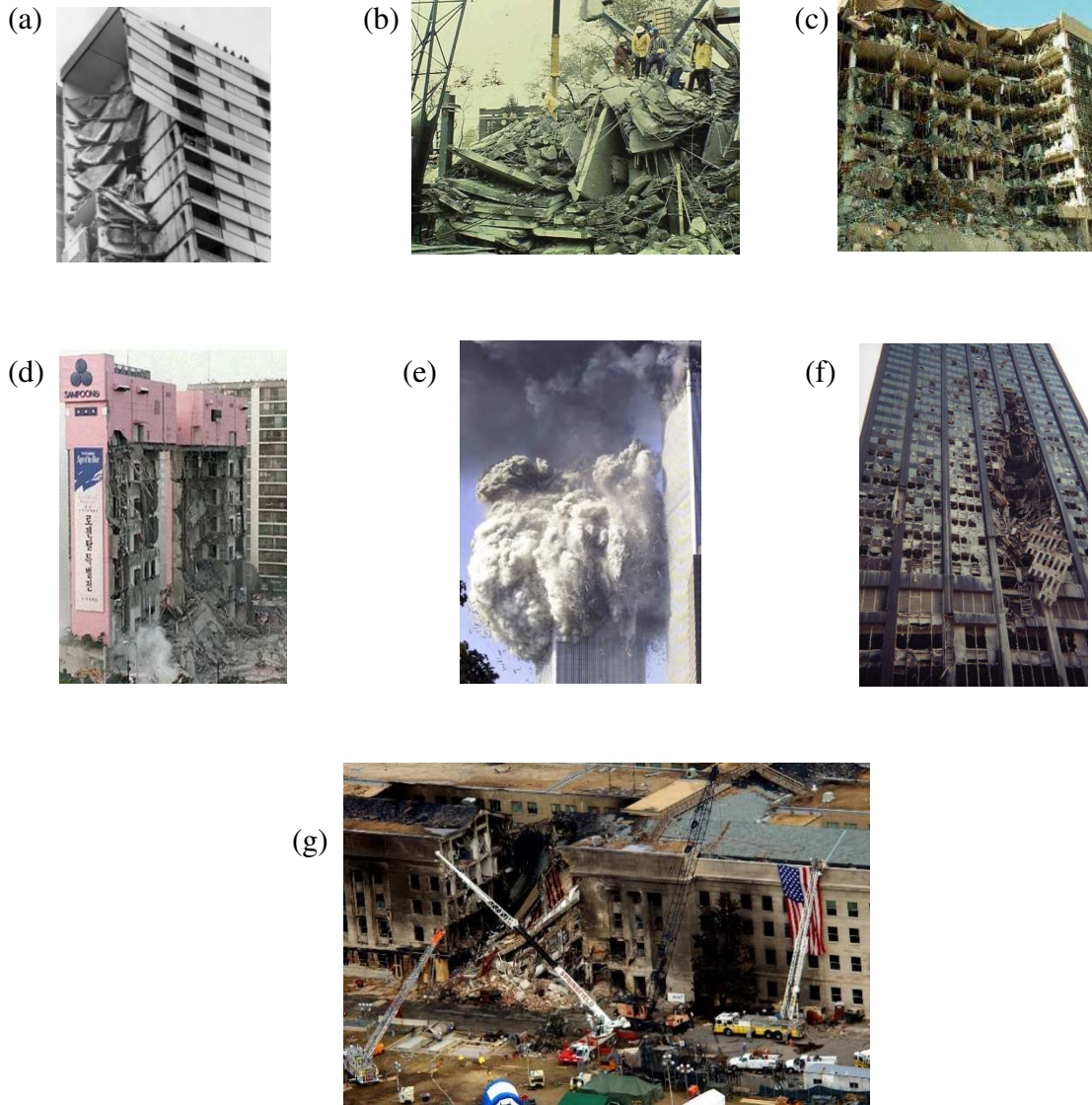


Figure 2.1 Cases of collapsed and non-collapsed buildings due to impacts,

- (a) Ronan Point apartment building (www.conspiromedia.wordpress.com),
- (b) L'Ambiance Plaza building (www.structuremag.org),
- (c) Alfred P. Murrah building (www.menwithfoilhats.com),
- (d) Sampoong Department Store building (www.theguardian.com),
- (e) World Trade Center Tower (www.telegraph.co.uk),
- (f) Bankers Trust building (www.attivissimo.net),
- (g) Pentagon building (www.publicintelligence.net).

2.2 Previous studies on progressive collapse

- **Between 1968 and 1975**

Study on the vulnerability of the building structures against progressive collapse was prompted after the collapse of the Ronan Point Apartment Building in 1968 due to the gas explosion in one of the apartments. Most of the research work was focused on the development of the relationship between the abnormal loads and progressive collapse, e.g., Astbury (1969), Burnett (1973), Mainstone (1973), and Burnett (1974). In order to prevent or to reduce the risk of the progressive collapse, several methods for considering the abnormal loads in the design were specified in the British Building Design Code. The 1975 edition of the National Building Code of Canada also made regulations on progressive collapse (Dusenberry 2002); however, no detailed guidance was provided. Meanwhile, many studies and workshops were held in the US during this time after the collapse of the Ronan Point Building. One of the studies that were given in Breen (1975) focused on the detailed design configurations of precast concrete structures against progressive collapse. Furthermore, development of the provisions of integral ties throughout the structure (indirect design) for the progressive collapse analysis was described in Breen (1975). Ferahian (1971) reviewed the changes made in the British and the Canadian codes on the progressive collapse analysis, and reported that earthquake design loads would have positive impact on protecting buildings from the progressive collapse. In addition, Popoff (1975) reviewed various types of connections and suggested the criteria for the minimum reinforcement of the design connections should be modeled in order to avoid progressive collapse.

- **Between 1976 and 1995**

A study conducted by Monsted (1979) showed the importance of primary components of a building (e.g., load-bearing walls) and connections in resisting the progressive collapse. He also investigated the effects of the alternative load path and catenary action after the failure of the load-bearing component on the collapse resistance. Webster (1980) proposed a methodology for determining the reliability of flat slabs in a multi-storey building. It should be noted that the objective of Webster's study was to reduce the risk of the progressive collapse during construction. Pekau (1982) performed a study on evaluating the behaviour of the precast panel shear walls during progressive collapse. The results from the study showed that failure of the exterior panel would lead to unexpectedly large shear forces, which would trigger the progressive collapse.

Gross (1983) conducted the first study on progressive collapse analysis of a steel moment-resisting frame building using two-dimensional finite element model. More specifically, nonlinear analyses were performed in which the nonlinearity of beams, columns, and connections were considered due to the failure of the columns. Shear effects of the infill panels were also taken into account in the numerical modelling. Casciati (1984) carried out a similar study on a reinforced concrete moment-resisting frame using 2D analysis. In order to consider the cyclic behaviour of the elements under seismic loading, Modified Takeda model was used to simulate the performance of plastic hinges at the ends of members. The study performed by Pretlove (1991) showed that fracture of a given member may cause overloading to the adjacent members which, in turn, would trigger the progressive collapse. He also questioned that the statically safe elements might not be reliable if dynamic effects were taken into account. It should be noted that sudden loss of

a column, by nature, is a dynamic mechanism. Unlike the relatively complicated analyses conducted in the studies mentioned above, Bennett (1988) proposed a simplified method to evaluate the potential of structures' progressive collapse. The alternative load path method was used in the study to evaluate the progressive collapse resistance of a space truss; both linear and nonlinear analyses were performed. Due to the large degree of static indeterminacy and sufficient redundancy in trusses, Bennet claimed that redistribution of forces would easily take place in a truss system after failure of an element. However, this conclusion has not always proven to be true (Murtha-Smith 1988).

It is necessary to mention herein that most of the studies performed during this period were based on several simplified assumptions and linear static analysis. However, it has been found later on that abnormal loads, which in most cases triggered the progressive collapse, were dynamic (i.e., not static) loads. In addition, the methodology for nonlinear analysis was not well developed at this time due to the lack of knowledge and constraints of computer science. Therefore, most of the results from these studies were not correct as explained in Lim (2004).

- **Between 1996 and 2010**

Astaneh-Asl (2001) did an experimental test on a typical steel building by removing a middle column on the building's perimeter in order to evaluate the progressive collapse resistance of the structure. Results from the test showed that the loads were well redistributed due to the catenary action of the steel deck and girders. Mlakar (2003) prepared a technical report on the investigation of the performance of the Pentagon Building under the attack of September 11, 2001. The results from the detailed finite element analysis showed that the building had a satisfactory performance overall even

though the columns on the first floor were extensively damaged. Furthermore, several factors attributed for preventing building structures from collapse were reported; some of them are summarized as follows,

- A frame system consisting of beams and girders could provide sufficient redundancy and alternative load path in case of the loss of the vertical load-bearing components.
- Shorter spans have advantages over longer spans in terms of progressive collapse resistance.
- Higher design loads (i.e., 150 psf or 7.18 kPa in excess of service loads) might be considered in the design of the building in order to resist the progressive collapse.
- Appropriate design detailings, such as continuity of the bottom reinforcement in the beams and girders extending into the supports, spiral reinforcement, could increase the progressive collapse resistance of the building.

During this period, a beam element formulation and solution was introduced for the dynamic progressive collapse analysis. According to this procedure, inelastic beam-column elements were formulated using the lumped plasticity approach with the concentrated inelasticity at the element ends (Kaewkulchai 2004). The results of this study showed that both the capacity of the structural members and the number of the plastic hinges could be underestimated if the dynamic effects were not considered in the progressive collapse analysis. It was also concluded in Kaewkulchai (2004) that static analysis might not provide conservative results on estimating the potential of the progressive collapse. Grierson et al. (2005) focussed a study on developing qualitative criteria for progressive collapse analysis. Based on the results from linear analyses in the

study, Grierson proposed simplified methods that can be implemented in the structural analysis software. Moreover, the results were verified by comparing them with those using nonlinear analyses. One year later, Kim and Park (2006) advanced the progressive collapse analysis by introducing a concept of Energy Balance, which was considered to have a great potential to simplify the analysis. A comprehensive study on the progressive collapse analysis was conducted by Kim et al. (2009). The examined buildings were moment-resisting steel frame buildings, and they were 3-, 6-, and 15-storey high, respectively. The buildings were designed for gravity loads only, and as such, the combination of the gravity and seismic loads were assessed in order to see the contribution of the seismic loads to the progressive collapse resistance.

Izzuddin et al. (2008) proposed a framework for progressive collapse analysis of tall buildings. They suggested that the ductility, redundancy and energy dissipation in the structural system should be considered in the event of a sudden failure of a column. Yagob et al. (2009) concluded that the overall response of existing RC buildings against progressive collapse can be improved by considering the local failures. Also, a need to review the available knowledge on the progressive collapse phenomenon has been remarked in this study.

- **Between 2011 and 2015**

Lin et al. (2011) conducted progressive collapse analyses on reinforced concrete frame buildings designed according to the seismic provisions of the 2005 edition of the National Building Code of Canada. In total, six buildings were considered in the study, in which three were in Ottawa and three were in Vancouver with heights of 5, 10, and 15 storeys, respectively. The performance of the buildings against progressive collapse was

evaluated according to the 2003 GSA which was available at that time. The Ottawa buildings were found to be more vulnerable to progressive collapse than the Vancouver buildings. The results from this study showed that the vulnerability of the progressive collapse of seismically designed buildings depended greatly on the differences between the spans of the longitudinal and the transverse frames, i.e., larger differences between the spans led to higher vulnerability.

Mirvalad (2013) investigated the vulnerability of progressive collapse of three steel moment-resisting frame buildings in Canada, which were located in different seismic hazard zones. Nonlinear dynamic analysis was conducted and the vulnerability of the buildings was evaluated based on 2003 GSA. Like the findings in Lin et al. (2011), Mirvalad also reported that steel buildings in low seismicity zones are more vulnerable to progressive collapse. Furthermore, two methods for retrofitting of the buildings with high vulnerability to progressive collapse were proposed in the study by using the top beam-girder system and the gravity truss system. Tran and Li (2014) studied the backbone curves of reinforced concrete columns with light transverse reinforcement by conducting experimental tests. Livingston et al. (2015) evaluated the response of a continuous beam by changing structural characteristics (e.g., yield strength of rebars, span length and axial stiffness) using a detailed finite element model. The collapse test of a three-storey reinforced concrete frame (half scale) was carried out by Xiao et al. (2015); failure mechanisms in addition to load-transfer path and the dynamic response, were discussed in the study. They concluded that the slabs and beams directly connected to the failed columns have significant effect on disproportionate collapse resistance. Moreover, the requirement of providing sufficient anchorage capacity to the joints should be provided in the guidelines

for the progressive collapse analysis in order to achieve the catenary action, which is beneficial for the collapse resistance.

2.3 Existing Guidelines

2.3.1 Overview of 2003 GSA

In June 2003, the US General Service Administration (GSA) released "Progressive Collapse Analysis and Design Guidelines for New Federal Office Buildings and Major Modernization Projects". The Guidelines were developed such that the potential of progressive collapse is taken into account in the design, planning and construction of new buildings and major renovation projects. More specifically, the GSA Guidelines are intended to:

- Assist in the reduction of the potential for progressive collapse in new Federal Office Buildings,
- Assist in the assessment of the potential for progressive collapse in existing Federal Office Buildings,
- Assist in the development of potential upgrades to facilities, if required,

Given this, the methodology proposed in GSA mainly focuses on the subsequent effects of the abnormal loading on the structure, which is known as threat-independent. Moreover, the requirements specified in GSA were developed to meet the provisions of the Security Criteria on the progressive collapse developed by the Interagency Security Committee (ISC). As stipulated in GSA, the Guidelines apply to "In-house government engineers, architectural/engineering (A/E) firms and professional consultants under contract to GSA as primary users. While mandatory for GSA facilities, these Guidelines

may also be used or adopt by any agency, organization or private concern."

Two methods were proposed in 2003 GSA, i.e., the simplified method and the advanced method, depending on the number of stories above the ground. More specifically, the simplified method is used for buildings less than 10 stories. Otherwise, the dynamic method must be used. For ease of discussion, the simplified method and the advanced method are referred to as the linear analysis method and the nonlinear analysis method, respectively, in this chapter. It is well known that nonlinear analysis method is more precise than linear analysis method since the nonlinearity of the material and geometry during the event of the progressive collapse is taken into account in the analysis. However, it should be noted that nonlinear modelling might be a big challenge for some of the projects.

GSA also addresses the need to protect human lives and prevent injuries in addition to protect the building and its functions. In order to evaluate the performance level defined in these guidelines, ASCE 41.13 (2014) specifies some structural and non-structural criteria for Damage Control and Building performance level (Table 2.1).

Table 2.1 Damage control and building performance levels – ASCE 41.13 (2014)

Overall damage	Target building performance levels			
	Collapse prevention	Life safety	Immediate occupancy	Operational
	Severe	Moderate	Light	Very light
General	<p>Little residual stiffness and strength, but load bearing column and walls function. Large permanent drifts. Some exits blocked. Infill and un-braced parapets failure or at incipient failure. Building is near collapse.</p>	<p>Some residual strength and stiffness left in all stories. Gravity load bearing elements function. No out of plane failure of walls or tipping of parapets. Some permanent drift. Damage to partitions. Building may be beyond economic repair.</p>	<p>No permanent drift. Structure substantially retains original strength and stiffness. Minor cracking of facades, partitions, and ceilings as well as structural elements. Elevators can be restarted. Fire protection operable.</p>	<p>No permanent drift. Structure substantially retains original strength and stiffness. Minor cracking of facades partitions, and ceilings as well as structural elements. All systems important to normal operation are functional.</p>

Table 2.2 Damage control and building performance levels (Continued).

Overall damage	Target building performance levels			
	Collapse prevention	Life safety	Immediate occupancy	Operational
	Severe	Moderate	Light	Very Light
Non-structural components	Extensive damage	Falling hazards mitigate but many architectural, mechanical and electrical systems are damaged.	Equipment and contents are generally secure, but may not operate due to mechanical failure or lack of utilities.	Negligible damage occurs. Power and other utilities are available, possibly from standby secure.
Comparison with performance intended for building designed under NEHRP provision, for design earthquake.	Significantly more damage and greater risk.	Somewhat more damage and slightly higher risk.	Less damage and lower risk	Much less damage and lower risk

The major performance levels defined in Table 2.1 are summarized below,

- **Immediate Occupancy Structural Performance Level (S-1):**

The risk of life-threatening injury as a result of structural damage is very low, and although some minor structural repairs may be appropriate, these would generally not be required prior to re-occupancy.

- **Life Safety Structural Performance Level (S-3):**

The overall risk of life-threatening injury as a result of structural damage is expected to be low. It should be possible to repair the structure; however, for economic reasons this may not be practical. While the damaged structure is not an imminent collapse risk, it would be prudent to implement structural repairs or install temporary bracing prior to re-occupancy.

- **Collapse Prevention Structural Performance Level (S-5):**

Significant risk of injury due to falling hazards from structural debris may exist. The structure may not be technically practical to repair and is not safe for re-occupancy, as aftershock activity could induce collapse.

To assist in using the Guidelines, a flow-chart methodology (Fig. 2.2) was given in GSA which helps to determine if the facility under consideration might be exempt from detailed consideration for progressive collapse. As seen in the figure, a number of questions should be answered to identify whether the progressive collapse analysis should be considered or not. These questions mainly include building occupancy, building category, seismic zone, number of stories, and the details about connections.

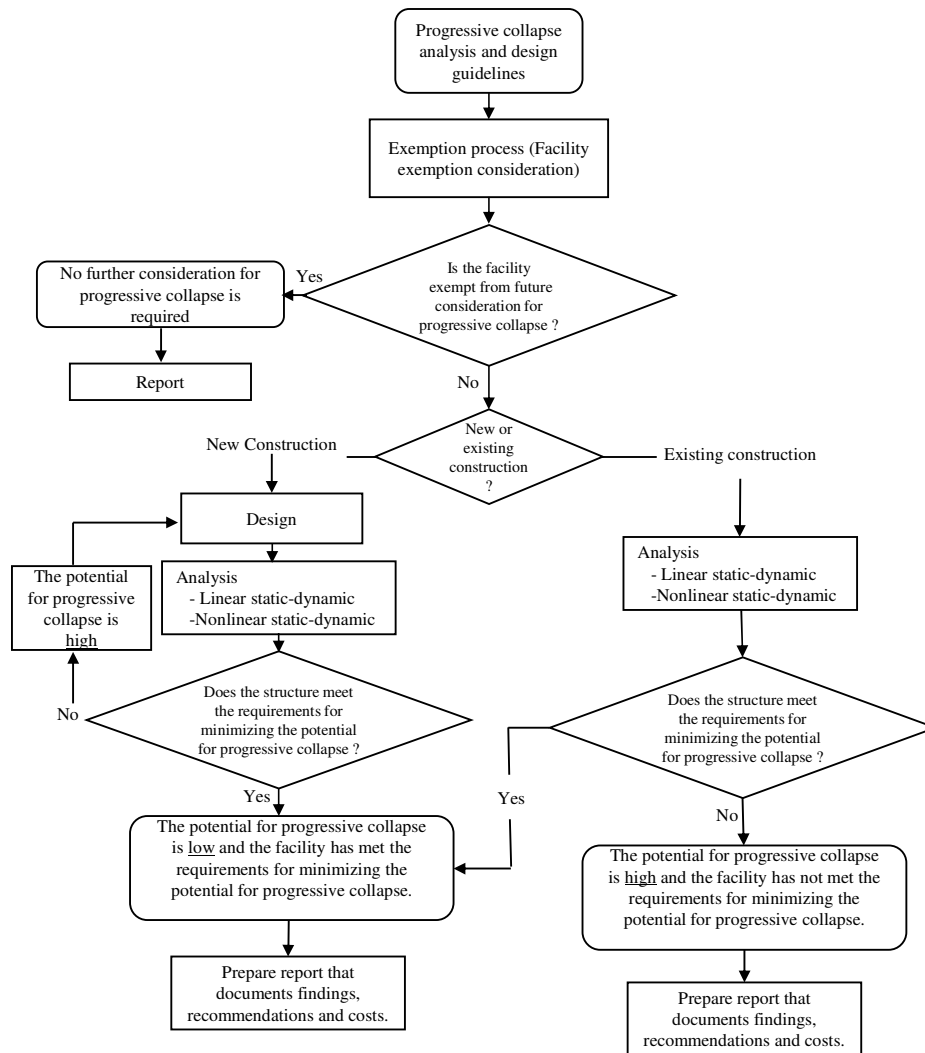


Figure 2.2 Overall flow for consideration of progressive collapse adopted from GSA (2003).

In general, the methods for progressive collapse analysis are divided into direct method and indirect method. The direct method includes "Alternative Path Method" and "Specific Load Resistance Method", while the indirect method includes "Minimum Levels of Strength, Ductility and Continuity" and "Tie Force Method" (NISTIR 7396). Among the methods mentioned above, GSA adopted the "Alternative Path Method". In this method, the demand on the entire load-bearing elements including beams, columns, foundations, etc., should be evaluated for different scenarios of the column or wall removal. The objective of the analysis is to make sure that the alternate load paths are available in a case of an element(s) failure. In a normal condition (i.e., the progressive collapse will not happen) for a building designed for gravity loads, the loads are first distributed over the slab, then they will be transferred to beams, and further transferred to the columns; finally, all the loads will be transferred to the foundation. However, in an abnormal condition (e.g., a building is attacked by a bomb explosion), if a column in a building lost its capacity, an alternate load path should be available such that the loads can still be transferred properly, i.e., no elements are overloaded. Furthermore, the Alternative Path Method requires that the structure be able to bridge over vertical load-bearing elements to be removed at a given location for the progressive collapse analysis.

In order to conduct progressive collapse analysis, critical locations for the column/wall removal should be defined first. This can be determined by engineering judgement. Nevertheless, GSA specifies three scenarios cases for the column/wall removal for regular structural configurations:

Case 1: the instantaneous loss of a column for one floor above grade (1st storey) located at or near the middle of the short side of the building.

Case 2: the instantaneous loss of a column for one floor above grade (1st storey) located at or near the middle of the longer side of the building.

Case 3: the instantaneous loss of a column for one floor above grade (1st storey) located at the center of the building.

The potential of progressive collapse of a given element is assessed by using the **Demand-Capacity Ratio (DCR)** if linear analysis is considered. The DCR ratio can be calculated using Equation 1,

$$DCR = \frac{Q_{UD}}{Q_{CE}} \quad (1)$$

Where,

Q_{UD} = **demand** (i.e., moment, axial force, or shear force acting on the member) resulting from the analysis, and

Q_{CE} = **capacity** of the member (i.e., moment, axial force, or shear force that the member can resist).

The loads used to determine the demand Q_{UD} are: $2(DL+0.25LL)$ for static analysis, and $DL+0.25LL$ for dynamic analysis, where DL represents the dead load, and LL represents the live load. The capacity Q_{CE} is determined based on the geometry and material properties of the section. The allowable DCR values for the structural members are $DCR \leq 2.0$ for regular buildings, and $DCR \leq 1.5$ for irregular buildings. If DCR ratios larger than the foregoing values are obtained, it indicates that the building has a high potential for progressive collapse.

2.3.2. Overview of 2013 GSA

The 2003 GSA Guidelines were replaced with a new edition in October 2013, which is referred to as 2013 GSA in this thesis. More specifically, the 2003 GSA was updated in order to keep consistency between the Interagency Security Committee (ISC 2013) Standards and GSA Guidelines in the level of building protection for progressive collapse. Furthermore, 2003 GSA Guidelines were modified such that its methodologies are similar to those specified in the Design of Buildings to Resist Progressive Collapse prepared by the Department of Defense (DoD 2005). Similar to 2003 GSA, the new 2013 Guidelines aim to reduce the potential for progressive collapse by bridging over the loss of the structural elements, limiting the extent of damage to a localized area (i.e., to make Alternative Paths available), and providing a redundant structural system along the height of the building. Moreover, 2013 GSA Guidelines address the need to save lives and prevent injuries as well.

In 2013 GSA, progressive collapse is defined as severe damage or collapse that is disproportionate to the magnitude of the initiating event. In fact, this definition focuses on the relative consequence or magnitude of collapse rather than the manner that triggers progressive collapse, as specified in 2003 GSA. Therefore, in practice, it is often referred to as "disproportionate" rather than "Progressive". Two threat-dependent approaches are given in the Guidelines;

- The first approach reduces the risk of progressive collapse for a defined threat by directly limiting the initial damage through hardening of structural elements.

- The second one reduces the risk of progressive collapse by limiting the propagation of initial damage, without explicit consideration the cause of the initial event, through implementation of Guidelines.

According to 2013 GSA, the application of the progressive collapse design depends on the required level of protection, which should be determined based on the number of stories and the Facility Security Levels (FSL) in accordance with ISC. There are five FSL levels specified in ISC, to ensure that security becomes an integral part of the planning, design and construction of new federal office buildings. It should be noted that progressive collapse design is not required for FSL I & II given the low occupancy and risk level associated with these types of facilities. However, the design is mandatory for FSL III & IV, and V; the details are as follows,

- FSL III & IV: for the buildings with four or more stories measured from the lowest point of exterior grade to the highest point of elevation. These facilities should implement both the Alternative Path and Redundancy Design Procedures.
- FSL V: 2013 GSA is applicable for all FSL V buildings regardless of the number of stories while the Redundancy Design Procedures do not need to be applied to these facilities.

Once a facility's FSL level has been determined, Guidelines can be applied by following the flow chart illustrated in Fig. 2.3.

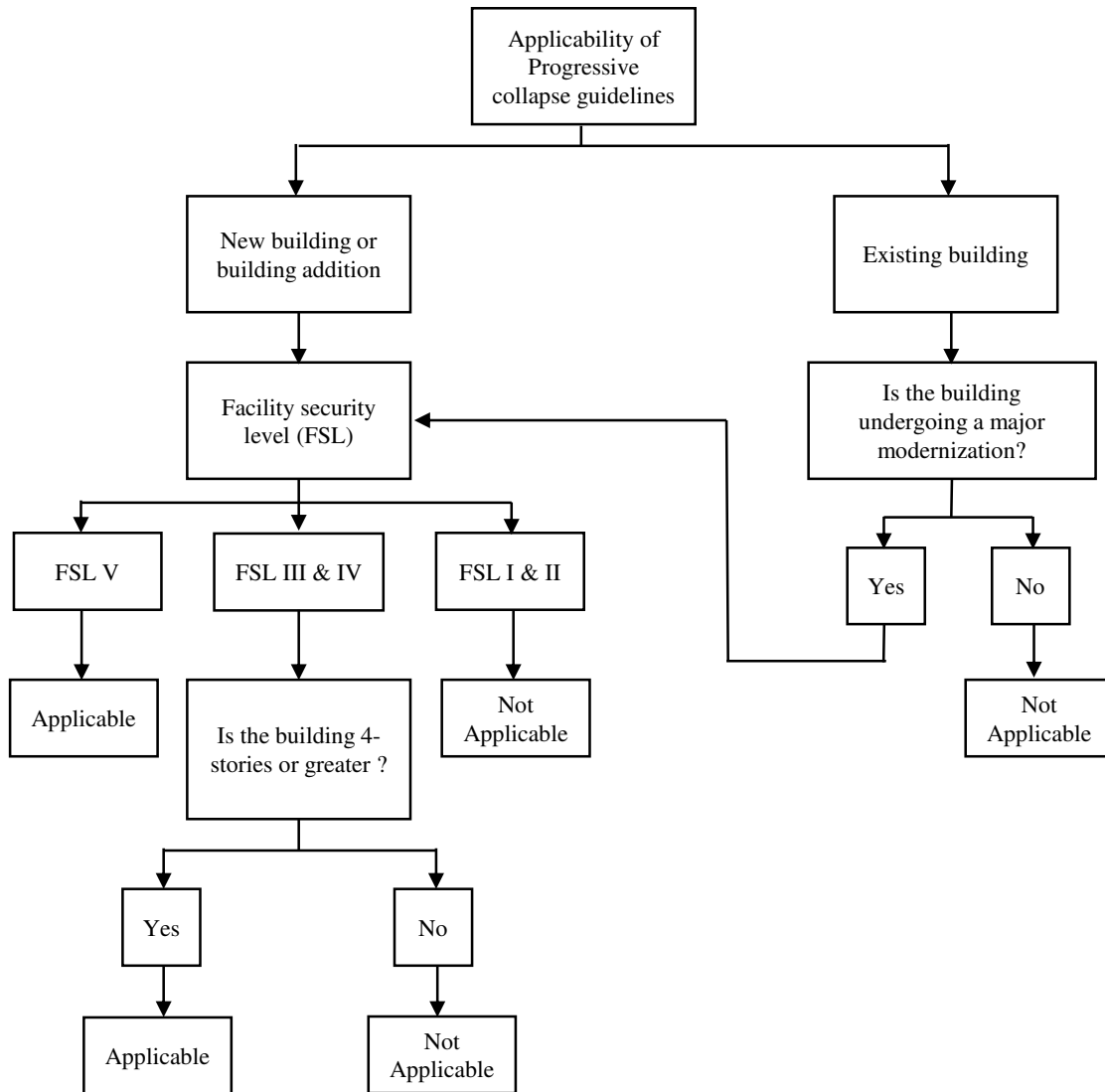


Figure 2.3 Applicability flow chart adopted from GSA (2013).

One of the major differences between 2003 GSA and 2013 GSA is the loads applied for the analysis. In order to simulate the behaviour of the structure after loss of load-bearing elements, both Guidelines suggested that the gravity loads should be increased for the purpose of the progressive collapse analysis. It is necessary to mention that the load increasing factor is used to take into account the dynamic effect during the column removal in static analysis. 2003 GSA recommends using a factor of 2 to amplify the gravity loads

on the areas mostly affected by the column removal for the static analysis. However, this factor was replaced by a factor Ω in 2013 GSA. This factor is not a fixed number; instead, it depends on the type of the structure, material, and analysis method.

2.4 Progressive collapse analysis

According to the 2013 GSA Guidelines, three types of analyses can be used in the assessment of the potential for progressive collapse of buildings, i.e., linear static analysis, nonlinear static analysis, and nonlinear dynamic analysis. For the purpose of the nonlinear analysis, including both dynamic and static, which is the most reliable method for the progressive collapse analysis, all the actions of the elements should be classified as either deformation- or force-controlled actions according to the Guidelines. The typical curves for the above-mentioned actions are illustrated in Fig. 2.4, in which the horizontal axis represents the deformation (i.e., rotation or displacement) while the vertical axis represents the moment or force. For a better understanding, Table 2.2 lists the typical examples of the deformation- and force-controlled actions defined in 2013 GSA. A detailed description of these two types of actions is given below,

- **Deformation-controlled actions:** significant ductile behaviour is expected for these actions. More specifically, an element or component behaves elastically until its yielding strength is reached, which is normally designated as f_y for a steel element or reinforcing steel under tension. When the yielding strength is exceeded, plastic hinges would be formed at the ends of the beams and/or columns. Referring to Fig. 2.4a, the elastic and plastic ranges are represented by the range between Points 0 and 1, Points 1 and 3, respectively. As illustrated in Figure 2.4, the plastic

range includes strain-hardening (between Points 1 and 2) and strength deterioration (between Point 2 and 3).

According to 2013 GSA, the action of a *primary* component is defined as deformation-controlled if $e \geq g$, where g and e represent the deformations at Points 1 and 2, respectively. Otherwise, the action should be classified as force-controlled, mainly because of the limited inherent ductility in such a *primary* element. On the other hand, the action of a *secondary* component is considered to be deformation-controlled for any e/g ratio.

- **Force-controlled actions:** brittle (i.e., non-ductile) behaviour is expected for these actions as shown in Fig. 2.4b. The component will lose its capacity once the yielding point (Point 1) is reached. Strictly speaking, this type of response should be avoided in the design of any type of structures. The components with force-controlled actions are just required to have strength capacity equal or larger than the demand, while neither rotation nor deformation is needed to be checked. Furthermore, performance level is not defined in GSA for these types of actions except for the end of the elastic stage.

Table 2.2 Examples of deformation- and force-controlled actions (GSA 2013).

Components	Deformation-controlled action	Force-controlled actions
Moment frames		
<i>Beams</i>	Moment (M)	Shear (V)
<i>Columns</i>	M	Axial load (P), V
<i>Joints</i>	--	V ¹
Shear walls	M,V	P
Braced frames		
<i>Braces</i>	P	--
<i>Beams</i>	--	P
<i>Columns</i>	--	P
<i>Shear links</i>	V	P, M
Connections	P, V, M ²	P, V, M

Note: ¹ Shear may be a deformation-controlled action in steel moment frame construction.

² Axial, shear, and moment may be deformation-controlled actions for certain steel and wood connections.

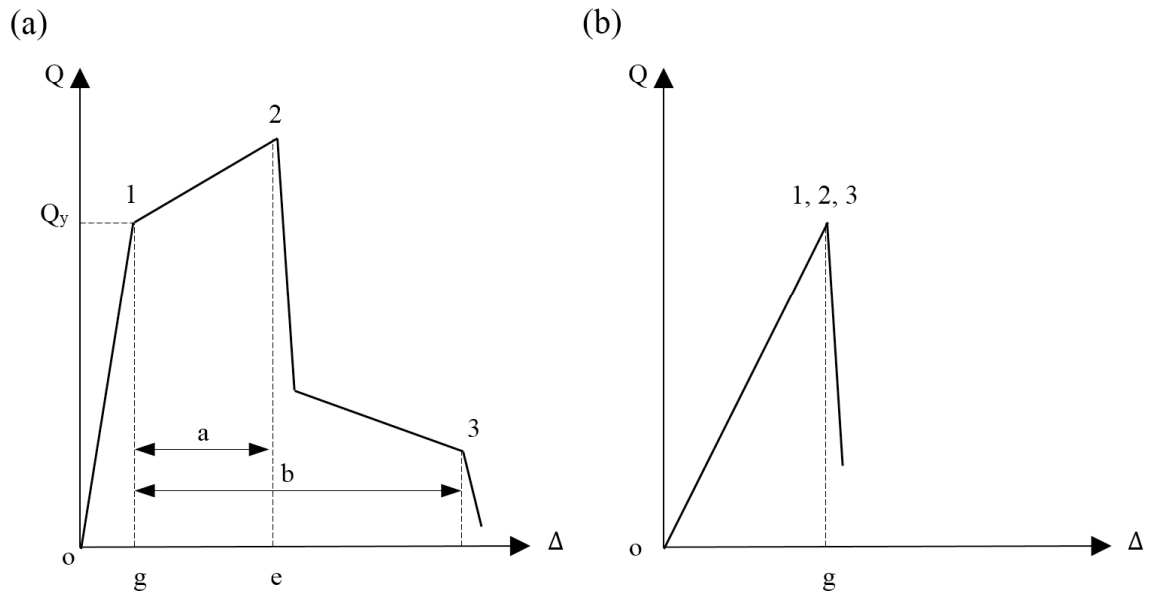


Figure 2.4 Definition of the actions adopted from GSA (2013), (a) Deformation-controlled actions, (b) Force-controlled actions.

According to 2013 GSA, the acceptance criterion for progressive collapse for deformation-controlled actions is that the maximum deformation should be within the elastic and plastic ranges, namely, between ordinates e and g as shown in Fig. 2.4a. The allowable deformations for the two ordinates are specified in GSA, and they depend on the expected performance level of the building after the event, namely, life safety and collapse prevention as described Section 2.3.1.

2.5 Summary

Studies on the progressive collapse are reviewed in this chapter. More specifically, comprehensive research on the experimental tests and analytical works between 1968 and 2015 is summarized in order to develop the originality of the work proposed in the thesis. The major requirements specified in the Guidelines published in 2003 and 2013 in the United States (2003 GSA and 2013 GSA) are also described in this chapter. The 2013 GSA Guidelines is commonly used by researchers and practitioners in North America for progressive collapse analysis.

Chapter 3

DESIGN OF RC MOMENT RESISTING FRAMES

3.1 Description of studied buildings

Typical 4-storey reinforced concrete office buildings in each of the following locations, i.e., Toronto, Montreal, and Vancouver, were designed for the purpose of the study. These locations were selected to represent the low, medium, and high seismic hazard zone in Canada, respectively. In each location, three span lengths were considered, namely, 4.0 m, 6.0 m, and 8.0 m in order to statistically analyze the relation between force and deformation of beams' end sections, which will be discussed in Chapter 4. The storey heights of all the buildings are 4.0 m. There are four spans in both the longitudinal and transverse directions. For illustration, Figure 3.1 shows the plan and elevation views of one examined building with a span length of 6.0 m. The lateral load resisting system consists of moment-resisting reinforced concrete frames in both the longitudinal and the transverse directions. There are five frames in the longitudinal direction (designated L_e and L_i in Fig. 3.1; L_e – exterior frames, and L_i – interior frames) and six frames in transverse direction (T_e and T_i). The floor system consists of a two-way slab supported by the beams of the longitudinal and transverse frames. The slab is cast integrally with the beams.

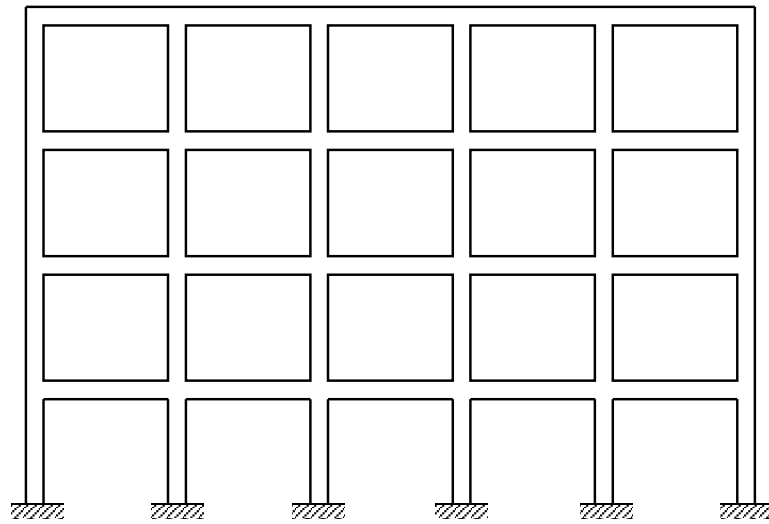
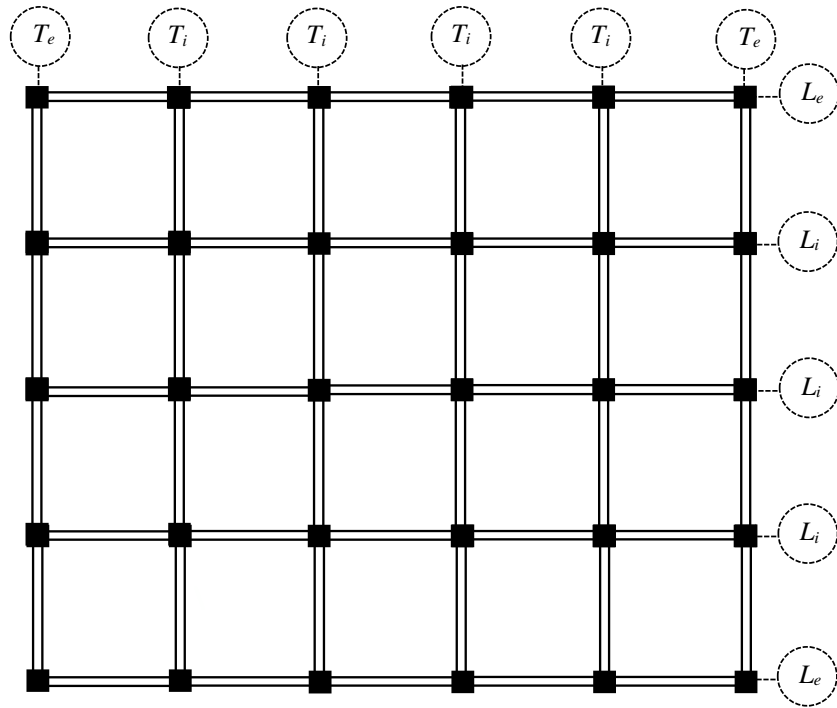


Figure 3.1 Plan of floors and elevation of longitudinal frames of the building (span = 6.0 m).

3.2 Design loads

3.2.1 Gravity loads

For the purpose of design, one of the interior longitudinal frames (Li) of the buildings was considered. The gravity loads were determined according to the 2010 edition of the National Building Code of Canada (NBCC 2010). More specifically, the superimposed dead load considered in the design was 2.0 kPa, which included the loads due to floor finishing, mechanical services, partitions, and suspended ceiling. The design live loads were 1.0 kPa and 2.4 kPa for the roof and floors, respectively. It is necessary to mention that snow loads were also considered in the design. As an example, Table 3.1 provides the design gravity loads for the frame with the span length of 6.0 m.

Table 3.1 Design gravity loads (kN/m²).

	Dead load		Live load
Roof	Weight of slab	3.75	
	Weight of beams	1.83	2.2
	Weight of columns	1.5	
	Superimposed	1.5	
	Total	8.58	2.2
Floor	Weight of slab	3.75	
	Weight of beams	1.83	2.4
	Weight of columns	1.5	
	Superimposed	2.0	
	Total	9.08	2.4

3.2.2 Seismic loads

The lateral loads due to earthquake ground motions were determined in accordance with NBCC using the equivalent static force procedure. 'Reference' ground conditions, represented by site class C in NBCC, were assumed at the building locations. The seismic

base shear force for each building, V , was computed according to the code formula (Equation 3.1):

$$V = \frac{S(T_a) \cdot M_V \cdot I_E \cdot W}{R_d R_o} \quad (3.1)$$

The minimum lateral earthquake shear force for moment-resisting frames, V_{\min} , should not to be less than that provided by Equation 3.2,

$$V_{\min} = \frac{S(2.0) \cdot M_V \cdot I_E \cdot W}{R_d R_o} \quad (3.2)$$

The maximum lateral earthquake shear force, V_{\max} should be calculated according to Equation 3.3,

$$V = \frac{2}{3} \cdot \frac{S(0.2) \cdot I_E \cdot W}{R_d R_o} \quad (3.3)$$

where, $S(T_a)$ is the design 5% damped spectral response acceleration at the fundamental lateral period of the building, M_V is the higher mode effect factor, I_E is the importance factor, W is the total seismic weight as defined by NBCC associated with the frame, R_d is the ductility-related force modification factor, and R_o is the overstrength-related force modification factor. The fundamental period of the frames was computed according to the code formula for reinforced concrete moment-resisting frames, $T_a = 0.075h_n^{3/4}$, where h_n is the height of the frame above the base in meters. The design spectral acceleration, $S(T_a)$, was determined from the seismic design spectrum for the building location (Fig. 3.2). The values of the other parameters used in Equation (3.1), as specified in NBCC, are: $M_V = 1$, $I_E = 1$. Given the seismicity of the building location, the frames in Toronto were designed as conventional frames (i.e., $R_d = 1.5$, $R_o = 1.3$); in Montreal they were designed as

moderately-ductile frames (i.e., $R_d = 2.5$, $R_o = 1.4$), and in Vancouver, were designed as ductile frames (i.e., $R_d = 4.0$, $R_o = 1.7$) in accordance with NBCC. The weight W includes the self-weight of the frame and the dead loads corresponding to the tributary areas acting on the frame at all floors, and 25% of the snow load is also added in the weight W . The design values for the fundamental periods of the building, T_a , the spectral accelerations, $S(T_a)$, and the base shear coefficients, V/W , are listed in Table 3.2.

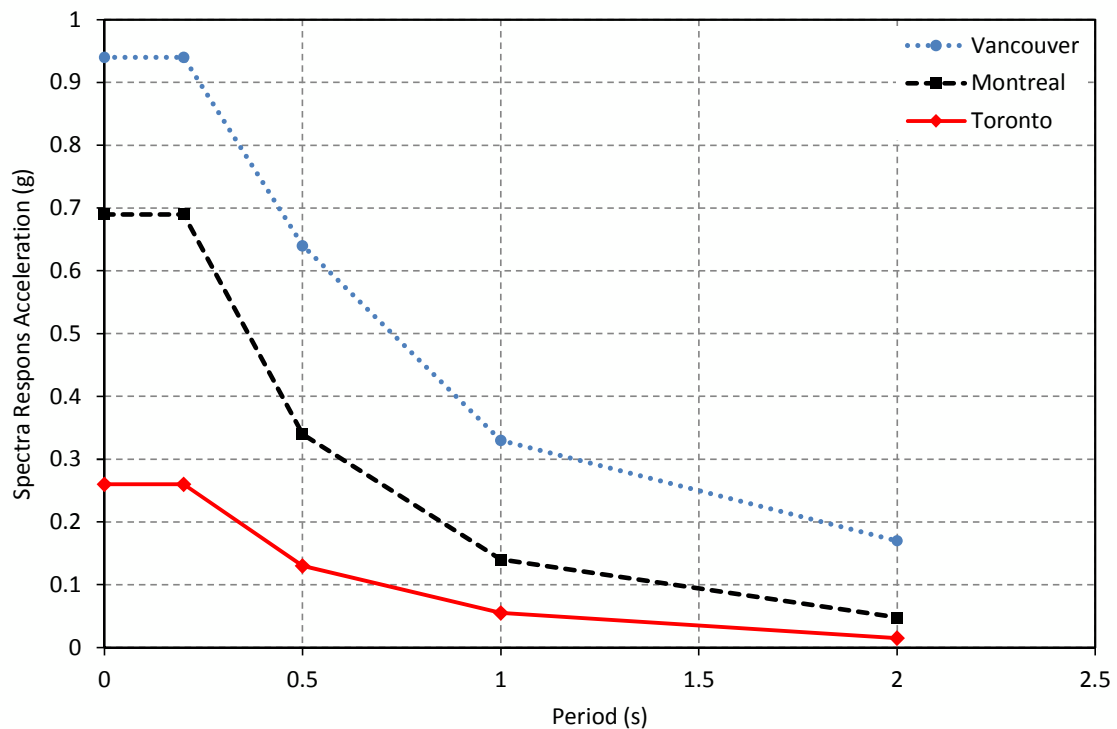


Figure 3.2 Seismic design spectra for Toronto, Montreal, and Vancouver, site class C, 5% damping.

Table 3.2 Design parameters for the buildings.

Design Parameter	Seismicity		
	Ductile	Moderately-ductile	Conventional
Fundamental period, T_a (s)	0.60	0.60	0.60
$S(T_a)$ (g)	0.54	0.28	0.10
V/W	0.088	0.171	0.307
Max. Drift (%)	0.348	0.388	0.265

For illustration of the results of the equivalent static force procedure, Figure 3.3 shows the distribution of the seismic shear force along the height of the frames in Toronto, Montreal, and Vancouver for the span length of 6.0 m. As expected, the shear force used for the design of the frame in Vancouver is more decreased than in Toronto and Montreal due to its relatively larger value for R_dR_o .

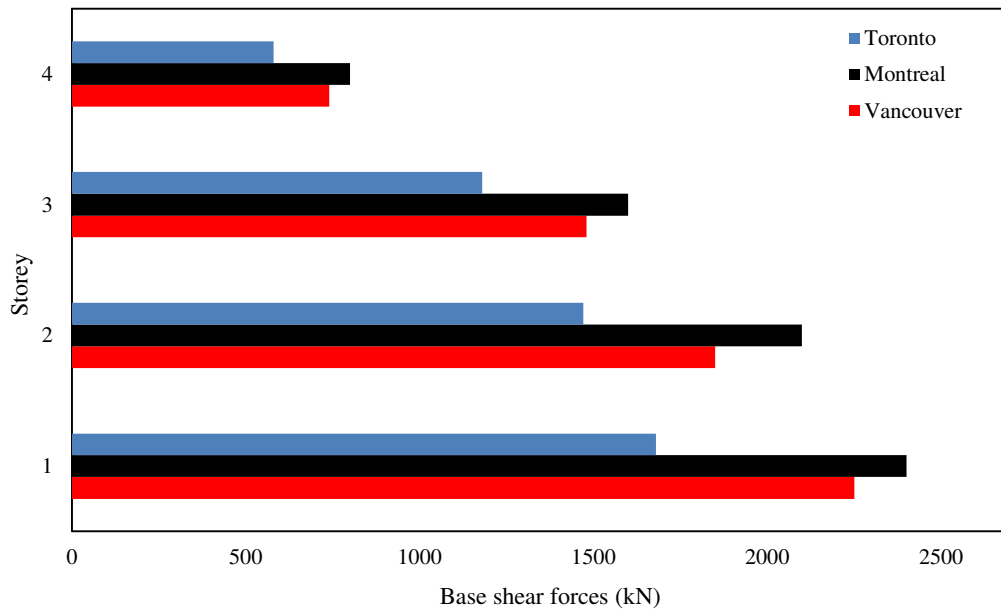


Figure 3.3 Distribution of the seismic force along the height of the building (span = 6.0 m).

3.3 Design of frames

The member forces for use in the design were determined by elastic analyses of the frames subjected to the combinations of gravity and seismic loads as specified in NBCC. The computer program ETABS was used in the analysis. Rigid zones were used at the beam-column joints of the structural model. The lengths of the rigid zones were selected to be the same as the depths of the beams and columns. The effects of cracking were included by using reduced member stiffnesses, i.e., 35% and 70% of the gross E_cI for beams and columns respectively, where E_c is the modulus of elasticity of concrete ($E_c = 28000$ MPa in this study), and I is the moment of inertia of the member section. The gross E_cI for the beams includes the slab thickness as specified in the Canadian standard CSA A23.3-14 (CSA 2014). Load-deflection (P- Δ) effects were taken into account in the analysis. As specified in NBCC, maximum inelastic inter-storey drifts were calculated as R_dR_o times the drift obtained from the elastic analyses. The maximum calculated drifts for the frames are given in Table 3.2. It can be seen that the calculated drifts are smaller than the design drift of 2.5% allowed by NBCC.

The member forces obtained from the elastic analyses were used in the design of the frames. The design was conducted in accordance with the requirements for the seismic design of frames specified in CSA standard A23.3-14 (CSA 2014). These requirements are based on the capacity design method. The capacity method intends to provide a strong column - weak beam frame structure in which the inelastic deformations due to strong seismic motions occur in beams rather than in columns. In the design, compressive strength of concrete is $f'_c = 40$ MPa, and yield strength of reinforcement is $f_y = 400$ MPa. The shear modulus of steel and concrete are defined to be 76.9 GPa and 12.1 GPa, respectively. The

dimensions of the longitudinal and transverse reinforcement of beams of buildings located in Toronto, Montreal, and Vancouver are shown in Tables 3.3, 3.4, and 3.5, respectively. A sample of the design is given in Appendix A. Furthermore, Figures 3.4, 3.5, and 3.6 illustrate the layout of the reinforcement in the beams for the three locations mentioned above.

3.4 Summary

For the purpose of the study, three types of RC moment frame buildings against seismic loads were designed according to 2010 NBCC, namely, conventional (Toronto buildings), moderately-ductile (Montreal buildings), and ductile (Vancouver buildings). In each location, nine frames were designed with the span lengths of 4.0 m, 6.0 m, and 8.0 m, and different reinforcement ratios (minimum, maximum, and the average between these two). Therefore, 27 frames were designed in order to propose moment-rotation curves for a wide range of the beams that will be discussed in Chapter 4.

Table 3.3 Dimensions and the longitudinal and transverse reinforcement of beams in Toronto.

Beam	Frame type	Span length (m)	Beam dimension (mm)	Transvers rebar plastic hinge region	Transvers rebar non hinge region	Longitudinal rebar in beams @ support				Longitudinal rebar in beams @ mid-span			
						Top (Tension)		Bottom (Compression)		Top (Compression)		Bottom (Tension)	
						Rebar	ρ	Rebar	ρ	Rebar	ρ	Rebar	ρ
C1*	Conventional	8.0	400 × 600	10M@200mm	10M@220mm	Minimum	0.5%	Minimum	0.2%	Minimum	0.0%	Minimum	0.2%
C2 (Design)	Conventional	8.0	400 × 600	10M@200mm	10M@220mm	1-15M+2-25M	0.5%	2-15M	0.2%	1-15M	0.1%	2-15M+1-25M	0.4%
C3	Conventional	8.0	400 × 600	10M@200mm	10M@220mm	1-30M+2M45	1.5%	2-30M	0.6%	1-30M	0.3%	2-30M+1-30M	0.9%
C4	Conventional	6.0	300 × 500	10M@200mm	10M@220mm	Minimum	0.7%	Minimum	0.3%	Minimum	0.1%	Minimum	0.5%
C5 (Design)	Conventional	6.0	300 × 500	10M@200mm	10M@220mm	1-10M+2-15M	0.3%	2-10M	0.1%	1-10M	0.1%	2-10M+1-15M	0.3%
C6	Conventional	6.0	300 × 500	10M@200mm	10M@220mm	1-20M+2M45	2.2%	2-25M	0.7%	1-20M	0.2%	2-25M+1-35M	1.3%
C7	Conventional	4.0	300 × 400	10M@200mm	10M@220mm	Minimum	0.3%	Minimum	0.2%	Minimum	0.3%	Minimum	0.2%
C8 (Design)	Conventional	4.0	300 × 400	10M@200mm	10M@220mm	1-10M+2-15M	0.4%	2-10M	0.2%	1-10M+2-15M	0.4%	2-10M+1-15M	0.3%
C9	Conventional	4.0	300 × 400	10M@200mm	10M@220mm	2-35M	1.7%	2-15M	0.3%	2-35M	1.7%	2-15M+1-30M	0.9%

*C stands for the Conventional beams.

Table 3.4 Dimensions and longitudinal and transverse reinforcement of beams in Montreal.

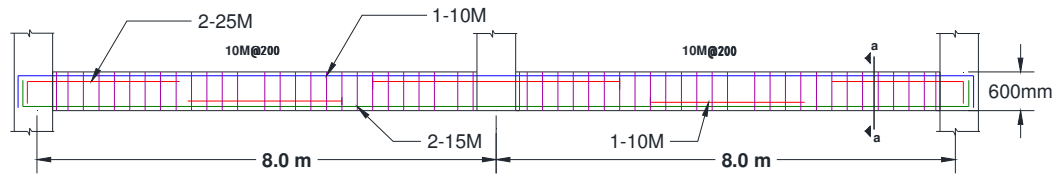
Beam	Frame type	Span length (m)	Beam dimension (mm)	Transvers rebar plastic hinge region	Transvers rebar non hinge region	Longitudinal rebar in beams @ support				Longitudinal rebar in beams @ mid-span			
						Top (Tension)		Bottom (Compression)		Top (Compression)		Bottom (Tension)	
						Rebar	ρ	Rebar	ρ	Rebar	ρ	Rebar	ρ
M1*	Moderately ductile	8.0	400 × 600	10M@100mm	10M@220mm	Minimum	0.5%	Minimum	0.2%	Minimum	0.1%	Minimum	0.3%
M2 (Design)	Moderately ductile	8.0	400 × 600	10M@100mm	10M@220mm	1-35M+2-20M	0.7%	2-25M	0.4%	1-35M	0.4%	2-25M	0.4%
M3	Moderately ductile	8.0	400 × 600	10M@100mm	10M@220mm	2-45M+1-45M	1.9%	2-45M	1.3%	1-45M	0.6%	2-45M	1.3%
M4	Moderately ductile	6.0	300 × 500	10M@100mm	10M@220mm	Minimum	0.3%	Minimum	0.1%	Minimum	0.1%	Minimum	0.1%
M5 (Design)	Moderately ductile	6.0	300 × 500	10M@100mm	10M@220mm	1-20M+2-25M	0.9%	2-20M	0.4%	1-20M	0.2%	2-20M+1-10M	0.5%
M6	Moderately ductile	6.0	300 × 500	10M@100mm	10M@220mm	1-30M+2-35M	1.8%	2-25M	0.7%	1-30M	0.5%	2-25M+1-30M	0.7%
M7	Moderately ductile	4.0	300 × 400	10M@100mm	10M@220mm	Minimum	0.3%	Minimum	0.2%	Minimum	0.1%	Minimum	0.2%
M8 (Design)	Moderately ductile	4.0	300 × 400	10M@100mm	10M@220mm	1-10M+2-20M	0.6%	2-20M	0.5%	1-10M+2-20M	0.6%	2-20M	0.5%
M9	Moderately ductile	4.0	300 × 400	10M@100mm	10M@220mm	1-25M+2-35M	2.1%	2-25M	0.8%	1-25M	0.4%	2-25M+1-20M	1.1%

*M stands for the Moderately ductile beams.

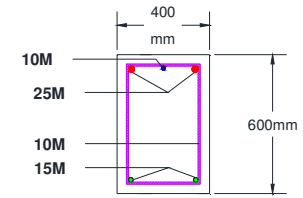
Table 3.5 Dimensions and longitudinal and transverse reinforcement of beams in Vancouver.

Beam	Frame type	Span length (m)	Beam dimension (mm)	Transvers rebar plastic hinge region	Transvers rebar non hinge region	Longitudinal rebar in beams @ support				Longitudinal rebar in beams @ mid-span			
						Top (Tension)		Bottom (Compression)		Top (Compression)		Bottom (Tension)	
						Rebar	ρ	Rebar	ρ	Rebar	ρ	Rebar	ρ
D1	Ductile	8.0	400 × 600	10M@100mm	10M@220mm	Minimum	0.3%	Minimum	0.2%	Minimum	0.2%	Minimum	0.2%
D2 (Design)	Ductile	8.0	400 × 600	10M@100mm	10M@220mm	1-30M+2-25M	0.7%	2-25M	0.4%	1-30M	0.3%	2-25M	0.4%
D3	Ductile	8.0	400 × 600	10M@100mm	10M@220mm	1-45M+2-45M	1.9%	2-35M	0.8%	1-45M	0.6%	2-35M+1-30M	1.1%
D4	Ductile	6.0	300 × 500	10M@100mm	10M@220mm	Minimum	0.5%	Minimum	0.1%	Minimum	0.1%	Minimum	0.2%
D5 (Design)	Ductile	6.0	300 × 500	10M@100mm	10M@220mm	1-25M+2-20M	0.7%	2-20M	0.4%	1-25M	0.3%	2-20M+1-10M	0.5%
D6	Ductile	6.0	300 × 500	10M@100mm	10M@220mm	1-30M+2-35M	1.8%	2-30M	0.9%	1-30M	0.5%	2-30M+1-15M	1.1%
D7	Ductile	4.0	300 × 400	10M@100mm	10M@220mm	Minimum	0.3%	Minimum	0.2%	Minimum	0.1%	Minimum	0.2%
D8 (Design)	Ductile	4.0	300 × 400	10M@100mm	10M@220mm	1-25M+2-15M	0.8%	2-15M	0.3%	1-25M	0.4%	2-15M	0.3%
D9	Ductile	4.0	300 × 400	10M@100mm	10M@220mm	25M+2-35M	2.1%	2-30M	1.2%	1-25M	0.4%	2-30M	1.2%

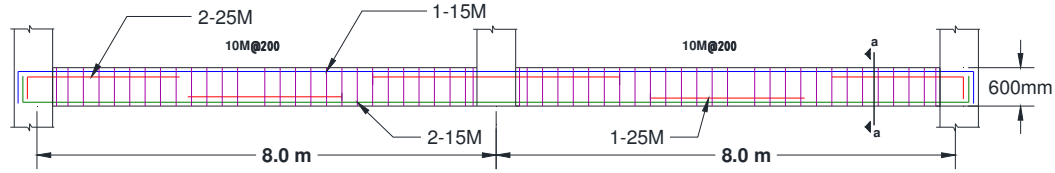
*D stands for the **D**uctile beams.



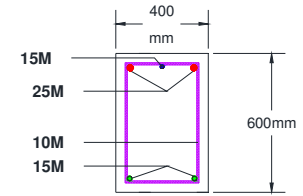
BEAM ELEVATION CASE C1



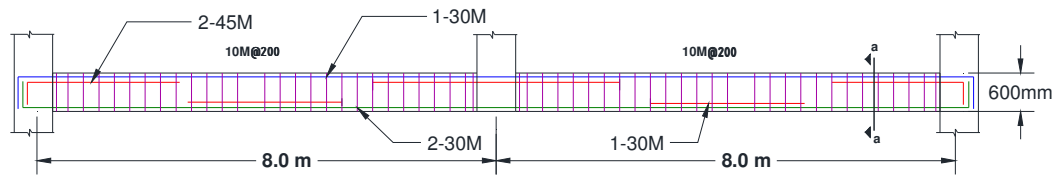
TYPICAL BEAM SECTION a-a



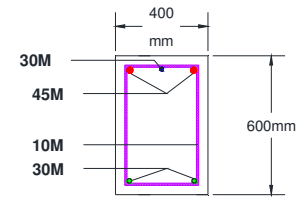
BEAM ELEVATION CASE C2



TYPICAL BEAM SECTION a-a

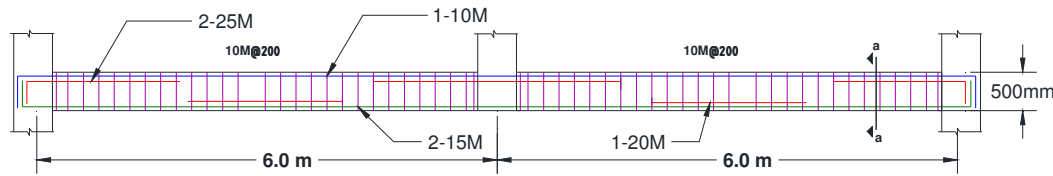


BEAM ELEVATION CASE C3

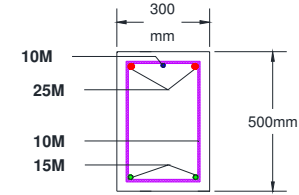


TYPICAL BEAM SECTION a-a

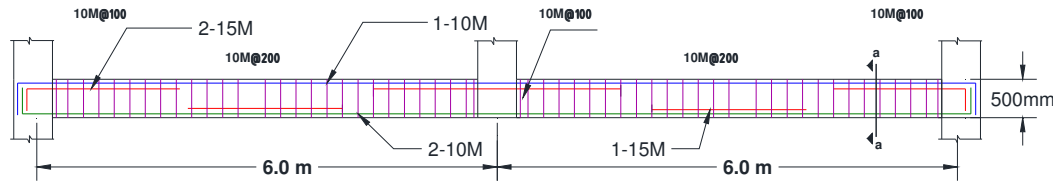
Figure 3.4 Layout of the reinforcement of the beams in Toronto.



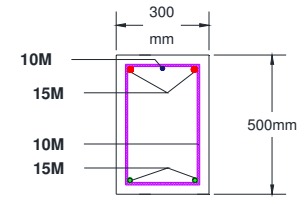
BEAM ELEVATION CASE C4



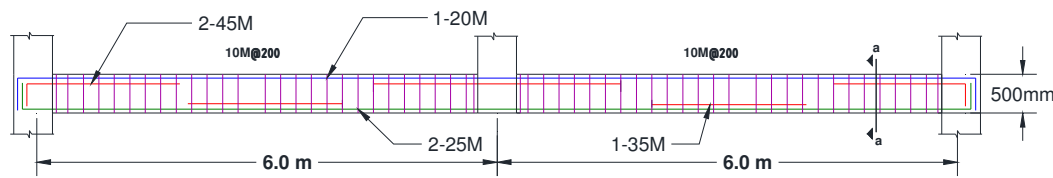
TYPICAL BEAM SECTION a-a



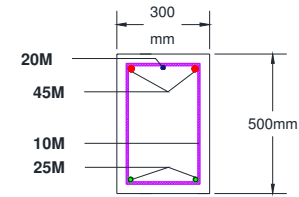
BEAM ELEVATION CASE C5



TYPICAL BEAM SECTION a-a

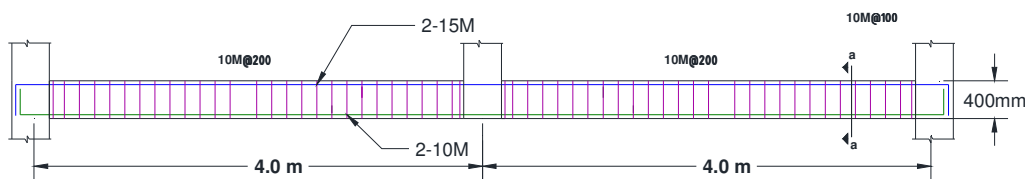


BEAM ELEVATION CASE C6

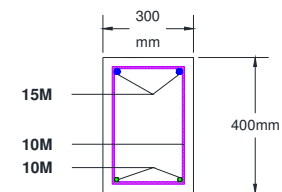


TYPICAL BEAM SECTION a-a

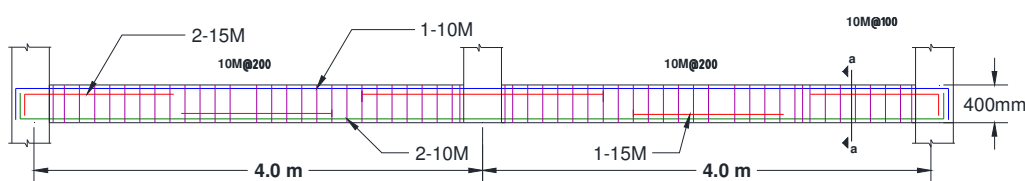
Figure 3.4 Layout of the reinforcement of the beams in Toronto (Continued).



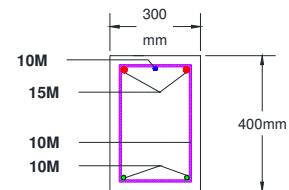
BEAM ELEVATION CASE C7



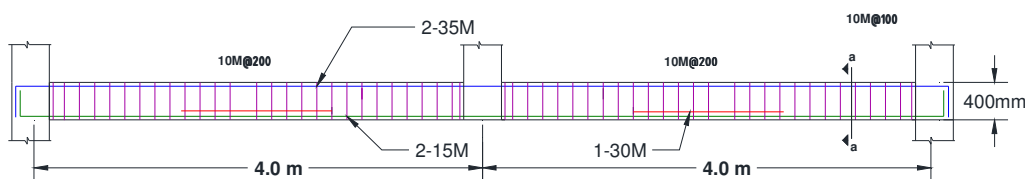
TYPICAL BEAM SECTION a-a



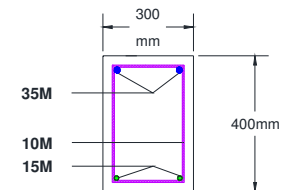
BEAM ELEVATION CASE C8



TYPICAL BEAM SECTION a-a

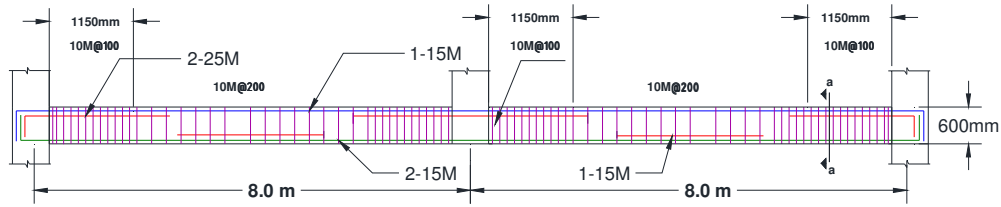


BEAM ELEVATION CASE C9

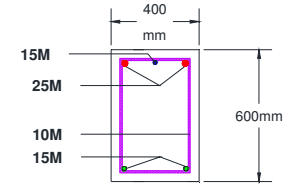


TYPICAL BEAM SECTION a-a

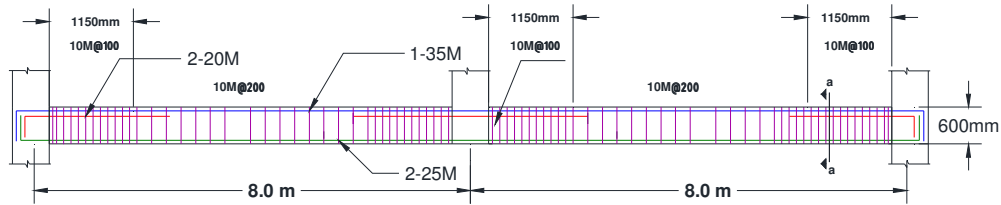
Figure 3.4 Layout of the reinforcement of the beams in Toronto (Continued).



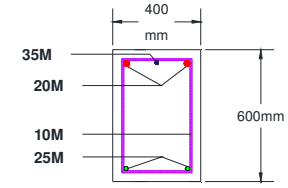
BEAM ELEVATION CASE M1



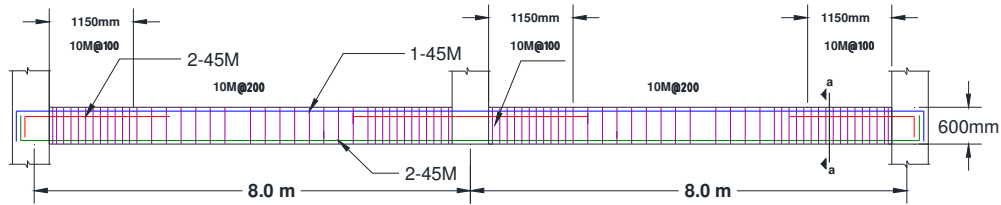
TYPICAL BEAM SECTION a-a



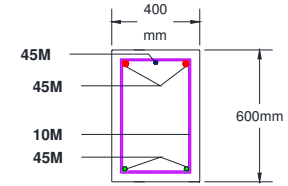
BEAM ELEVATION CASE M2



TYPICAL BEAM SECTION a-a

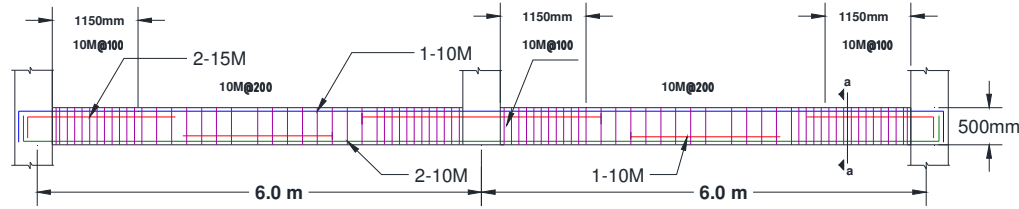


BEAM ELEVATION CASE M3

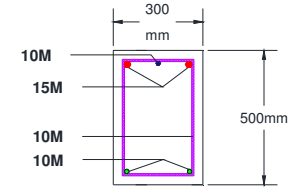


TYPICAL BEAM SECTION a-a

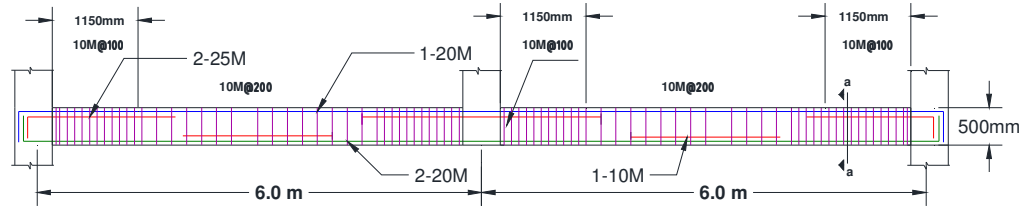
Figure 3.5 Layout of the reinforcement of the beams in Montreal.



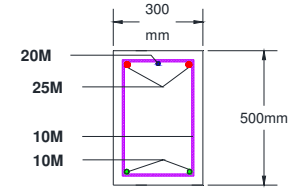
BEAM ELEVATION CASE M4



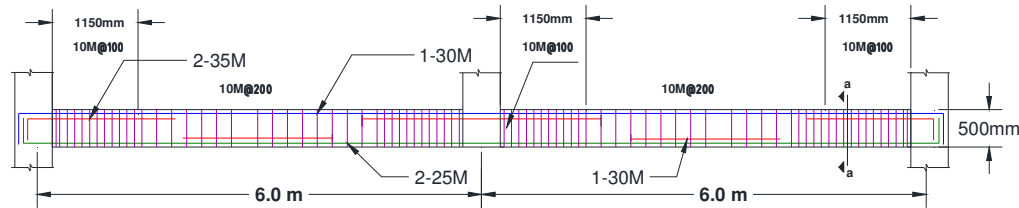
TYPICAL BEAM SECTION a-a



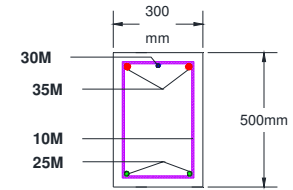
BEAM ELEVATION CASE M5



TYPICAL BEAM SECTION a-a

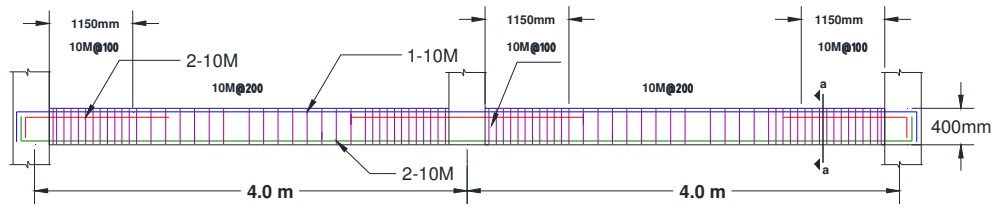


BEAM ELEVATION CASE M6

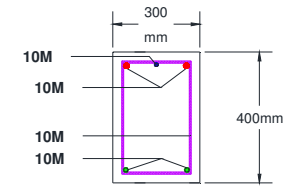


TYPICAL BEAM SECTION a-a

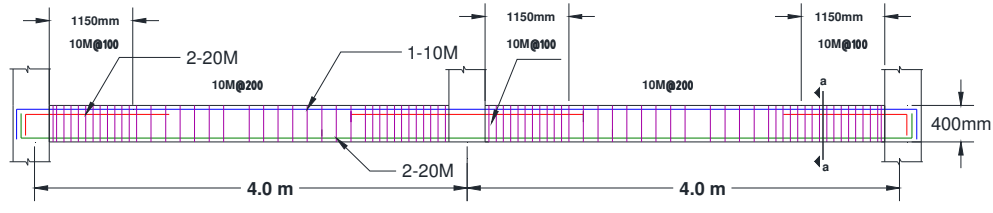
Figure 3.5 Layout of the reinforcement of the beams in Montreal (Continued).



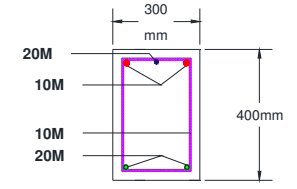
BEAM ELEVATION CASE M7



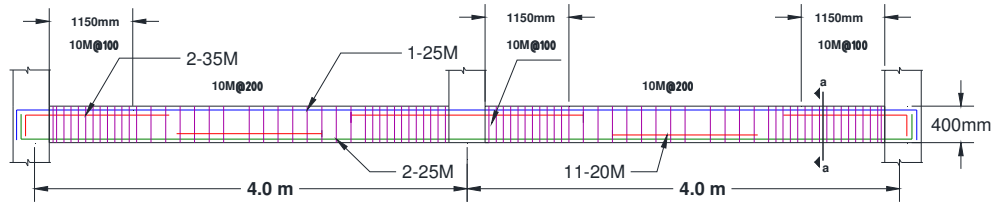
TYPICAL BEAM SECTION a-a



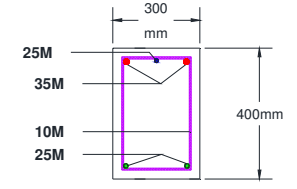
BEAM ELEVATION CASE M8



TYPICAL BEAM SECTION a-a

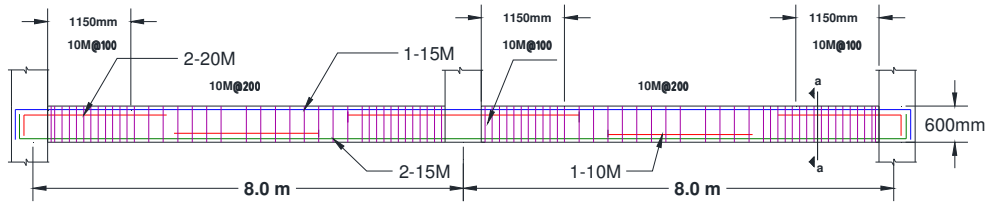


BEAM ELEVATION CASE M9

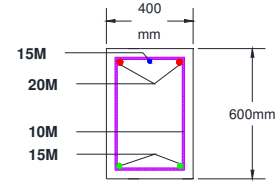


TYPICAL BEAM SECTION a-a

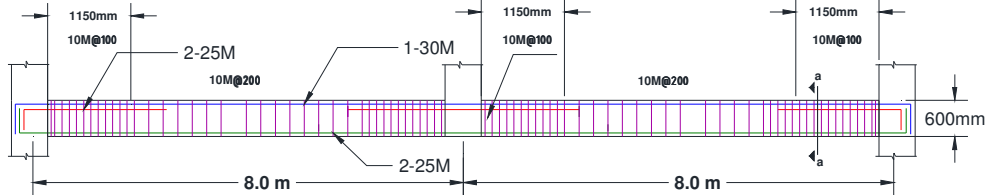
Figure 3.5 Layout of the reinforcement of the beams in Montreal (Continued).



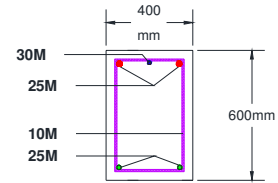
BEAM ELEVATION CASE D1



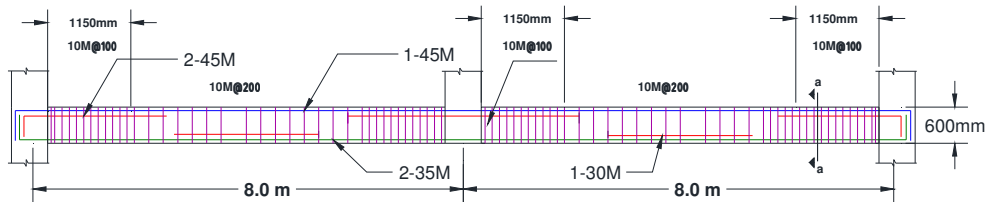
TYPICAL BEAM SECTION a-a



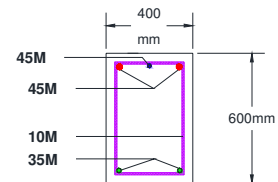
BEAM ELEVATION CASE D2



TYPICAL BEAM SECTION a-a

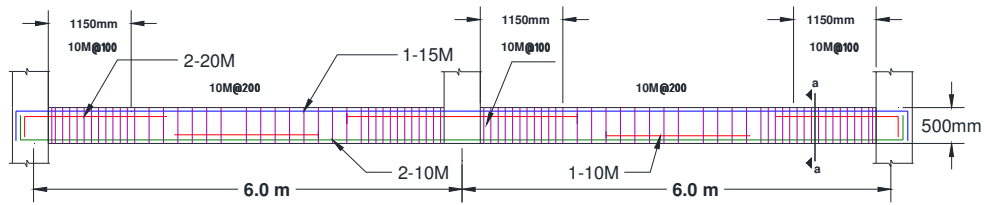


BEAM ELEVATION CASE D3

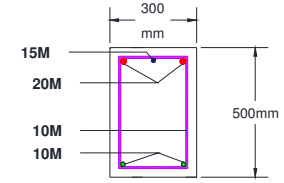


TYPICAL BEAM SECTION a-a

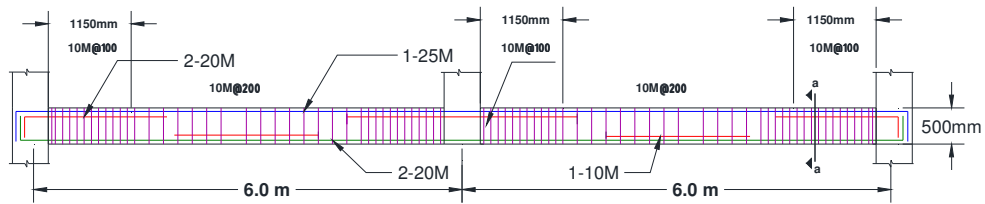
Figure 3.6 Layout of the reinforcement of the beams in Vancouver.



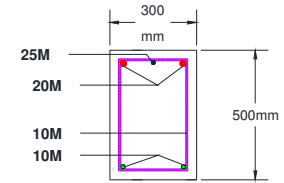
BEAM ELEVATION CASE D4



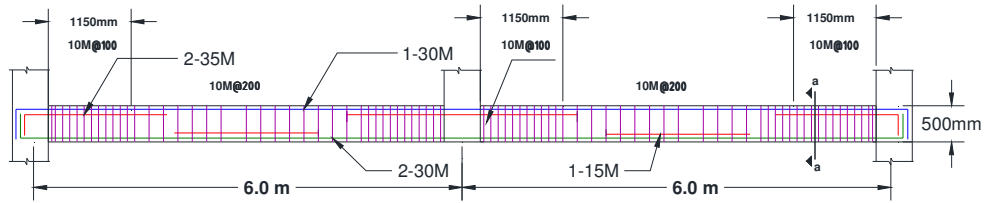
TYPICAL BEAM SECTION a-a



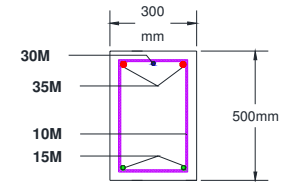
BEAM ELEVATION CASE D5



TYPICAL BEAM SECTION a-a

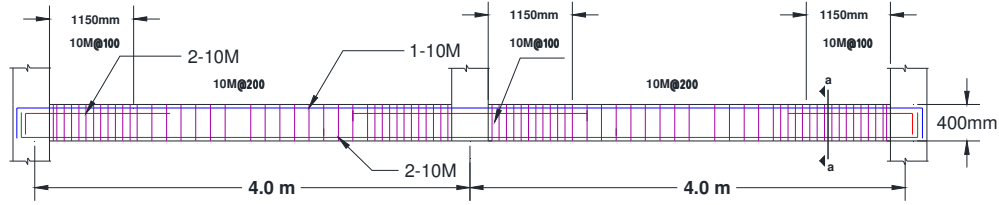


BEAM ELEVATION CASE D6

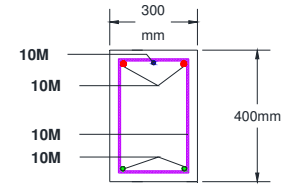


TYPICAL BEAM SECTION a-a

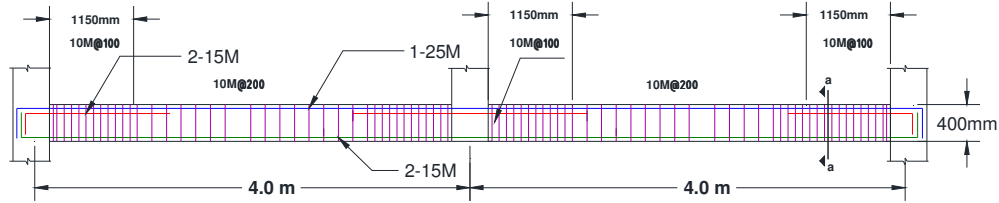
Figure 3.6 Layout of the reinforcement of the beams in Vancouver (Continued).



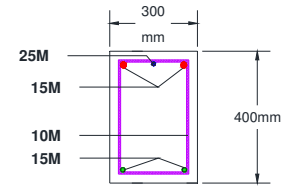
BEAM ELEVATION CASE D7



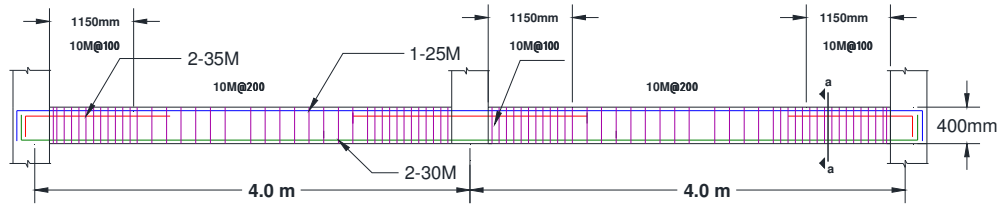
TYPICAL BEAM SECTION a-a



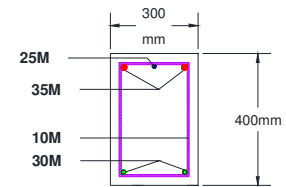
BEAM ELEVATION CASE D8



TYPICAL BEAM SECTION a-a



BEAM ELEVATION CASE D9



TYPICAL BEAM SECTION a-a

Figure 3.6 Layout of the reinforcement of the beams in Vancouver (Continued).

Chapter 4

PROPOSED MODEL FOR RC BEAMS' PLASTIC HINGES

4.1 Introduction

It is known that nonlinear dynamic analysis is the most suitable method for evaluating the performance of building structures against progressive collapse. To perform nonlinear analysis, parameters for modeling the plastic hinges that might be developed due to the column removal should be defined in accordance with 2013 GSA. As described previously, the objective of this study is to investigate appropriateness of the modelling parameters provided in GSA. Given this, three-dimensional (3D) finite element models of the designed buildings described in Chapter 3 were developed using the commercial software ABAQUS to accurately assess the geometric and material nonlinearity that occurred in the beams during the removal of the column. More specifically, nonlinear pushdown analysis was conducted on the interior frame C by increasing the displacement (downward) at the joint C3 (Fig. 4.1) where the column is removed until the beam collapses. It should be noted that ABAQUS has been used in numerous studies on evaluating the performance of RC beams (e.g., Sinaei et al. 2012, Deng et al. 2015, Liu et al. 2015, etc.). Other software, such as ANSYS has been also used to simulate nonlinear behaviour of concrete beams subjected to column removal (e.g., Sasani and Kropelnicki 2008, Valipour and Foster 2010, etc.)

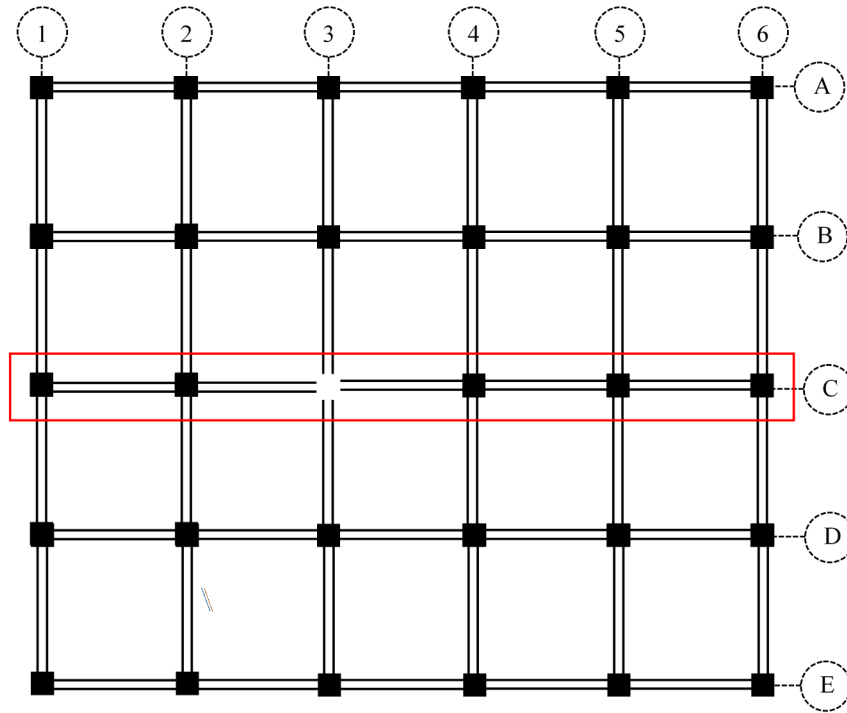


Figure 4.1 Critical frame with column removal.

4.2 Modelling techniques

4.2.1 Elements

Figure 4.1 schematically shows the 3D model developed using ABAQUS for the beam-column assembly, in which one of the columns is removed. Beams and columns were modelled using 3D deformable homogeneous solid element C3D8R (i.e., **C**ontinuum, **3-D**, **8**-node, **R**educed integration). The C3D8R element, with a good mesh, provides results with a high level of accuracy and less computation time (ABAQUS Analysis user's manual). Each node has three degrees of freedom along the x, y, and z axes.

It is necessary to mention that failure of side columns, and the beam-column joint, is not considered in the current ABAQUS model mainly because of the strong column-weak beam criteria adopted in current seismic design standards. Accordingly, the plastic hinges are expected to form in the beams, not in the columns. All the columns are modelled as fixed-fixed in axial, flexural and shear reactions. Beam-column joints are also assumed to be rigid, i.e., the joint undergoes the equal rotation of the corresponding beam. Equal sizes of the meshes are defined in beam-column faces in order to provide the connection between mesh edges.

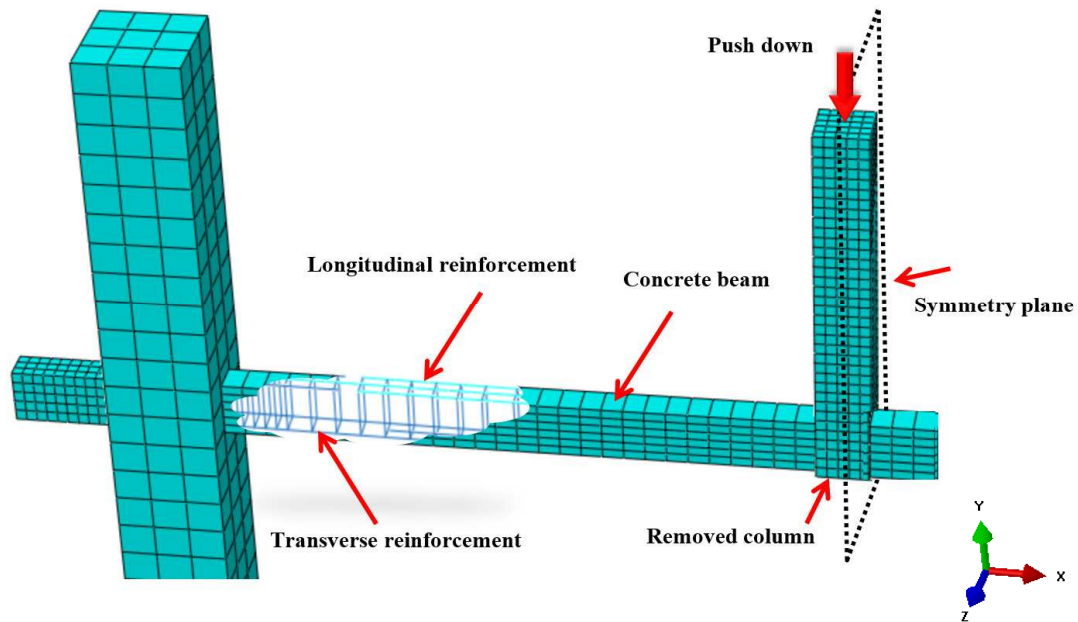


Figure 4.2 Schematic 3D ABAQUS model of the studied beam-column assembly.

4.2.2 Steel bars

Steel bars are modeled using 3D truss element T3D2 defined in ABAQUS, which can take tensile or compressive loads. T3D2 is a 3D spar element having two nodes with three-degrees of freedom at each node (i.e., translation in the x, y and z direction). A perfect

bond is assumed between concrete and steel bars. The longitudinal and transverse reinforcement developed in ABAQUS are shown in Fig. 4.2. Note that the detailing of the steel bars, e.g., location of longitudinal and transverse reinforcement, and the corresponding diameters were defined to be the same as those given in the design illustrated in Figs. 3.4 to 3.6 in Chapter 3. At the location where longitudinal and transverse rebars intersect, penetration of rebars is assumed; therefore, no extra interaction is required to connect them at points of intersection. Previous researchers (e.g., Bao et al. 2015, Ahmed 2014, Yu and Tan 2013, etc.) used similar approaches in modeling the beam reinforcement.

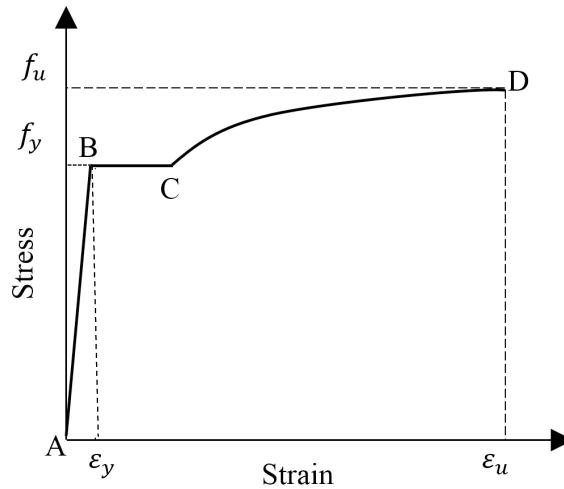


Figure 4.3 Stress-strain curve for the longitudinal and transverse steel bars.

Figure 4.3 presents the stress-strain curve for the steel bars (for both tensile and compressive) used in developing ABAQUS models in this study. It can be seen in the figure that the curve consists of three segments that represent the behaviour of the steel at three stages, namely elastic (AB), plastic (BC), and strain hardening (CD). Elastic strain is developed before steel reaches its yielding strength f_y (i.e., Point B), and it will be fully recovered while unloading. Once the strain exceeds the yielding strain ϵ_y , steel will go into

the plastic stage, i.e., uncovered deformations are developed. In general, permanent deformations are generated in steel followed by strain hardening. In this study, fracture of steel bars is assumed to occur when a failure strain of 0.2 is reached.

4.2.3 Concrete

The typical stress-strain relationship used for concrete material under tension and compression is shown in Fig. 4.4. The curve for compressive concrete is adopted from the model developed by Kent and Park (1971) and it is applicable for both unconfined and confined concrete. As seen in the figure, the curve for both unconfined and confined concrete has two branches, i.e., an ascending branch and a descending branch. Moreover, the curve for the ascending branch is the same for unconfined and confined concrete, which is represented by a second-order parabolic function. However, the descending branch is different, i.e., the unconfined concrete follows linear function while the confined concrete follows parabolic function. The stress of concrete for the ascending branch can be determined using Equation 4.1 while that for the descending branch can be determined using Equation 4.2. The parameter Z in Equation 4.2 should be calculated based on Equations 4.3 to 4.6 depending on the type of the concrete, i.e., unconfined and confined concrete.

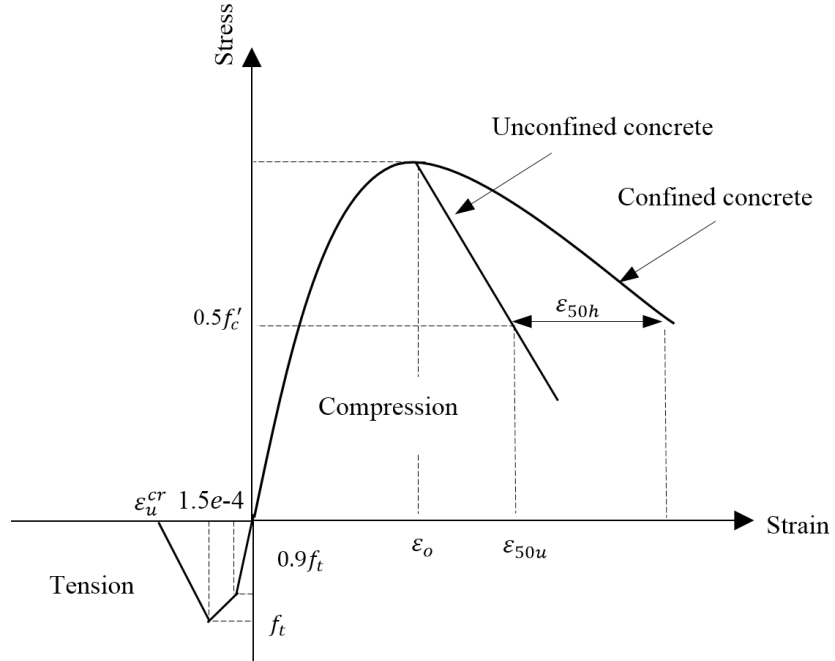


Figure 4.4 Stress-strain curve for concrete under compression and tension.

$$f_c = f_c' \left[\frac{2\varepsilon_c}{\varepsilon_{co}} - \left(\frac{\varepsilon_c}{\varepsilon_{co}} \right)^2 \right] \quad (4.1)$$

$$f_c = f_c' [1 - Z(\varepsilon_c - \varepsilon_{co})] \quad (4.2)$$

$$Z = \frac{0.5}{\varepsilon_{50h} - \varepsilon_{co}} \quad (\text{Unconfined concrete}) \quad (4.3)$$

$$Z = \frac{0.5}{\varepsilon_{50h} + \varepsilon_{50u} - \varepsilon_{co}} \quad (\text{Confined (concrete)}) \quad (4.4)$$

$$\varepsilon_{50u} = \frac{3 + 0.29f_c'}{145f_c' - 1000} \quad (4.5)$$

$$\varepsilon_{50h} = \varepsilon_{50c} - \varepsilon_{50u} \quad (4.6)$$

CEB-FIP (1991) proposed a bilinear curve for uncracked concrete subjected to tension as defined in Equation 4.7, which can be used to the ascending branch of the tensile curve. The cracked concrete follows a straight descending line in order to approximate the descending branch of tensile behaviour.

$$\sigma_{ct} = \begin{cases} E_{ci} \varepsilon_{ct} & 0 < \varepsilon_{ct} < 0.9 \frac{f_t}{E_{ci}} \\ f_t - 0.1 f_t \frac{0.00015 - \varepsilon_{ct}}{0.00015 - 0.9 \frac{f_t}{E_{ci}}} & 0.9 \frac{f_t}{E_{ci}} < \varepsilon_{ct} < 0.00015 \end{cases} \quad (4.7)$$

4.2.4 Cracking and failure of concrete

It is known that RC structures crack at small loads due to the low tensile strength of concrete. Furthermore, structures become soft when cracking occurs. To consider the effects of cracking on the performance of structures, three models are defined in ABAQUS, which are the **C**oncrete **S**meared **C**rack model (**CSC**), **B**rittle **C**racking model for **C**oncrete (**BCC**) and **C**oncrete **D**amaged **P**lasticity model (**CDP**). In this study, the CDP model was selected to simulate cracking and post failure of concrete.

The CDP model follows the concepts of isotropic damage elasticity with isotropic tensile and compressive plasticity. The two major failure mechanisms considered in the model are concrete compressive crushing and tensile cracking. Figures 4.5a and 4.5b illustrate the response of concrete subjected to uniaxial loading in tension and compression, respectively, which are specified in ABAQUS. As seen in Fig. 4.5a, under uniaxial tension, the stress-strain response of concrete follows a linear (i.e., elastic) relationship until the

failure stress, σ_{t0} , is reached, which corresponds to the onset of micro-cracking in concrete. Beyond σ_{t0} , micro cracks become macro (i.e., relatively larger) with a softening stress-strain response, and it leads to the formation of strain localization. Whereas under uniaxial compression (Fig. 4.5b), the response is elastic until the yield stress, σ_{c0} . Then the response is plastic, characterized by strain hardening followed by strain softening beyond the ultimate stress, σ_{cu} .

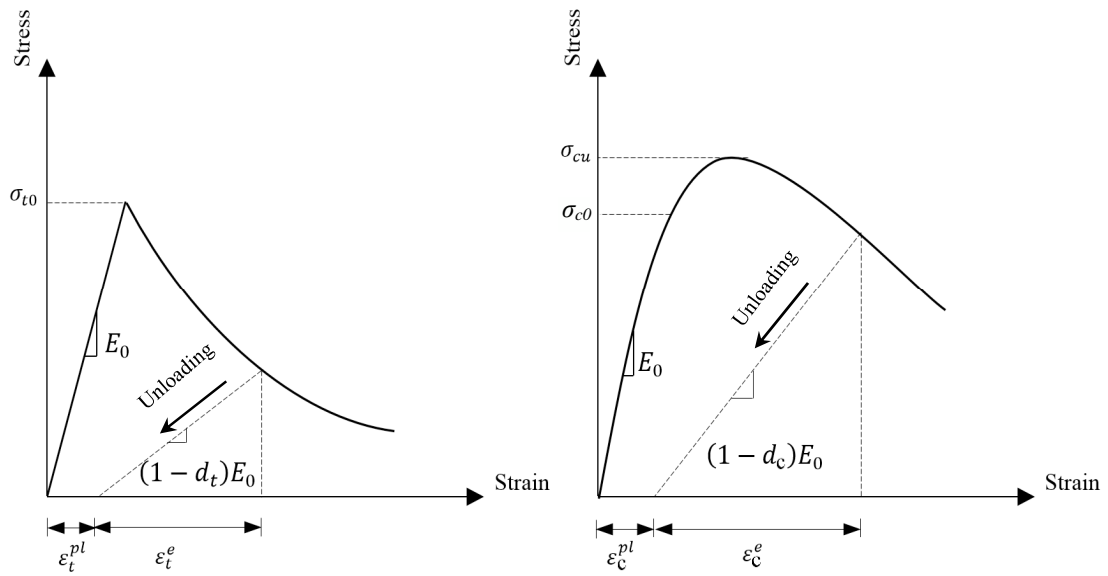


Figure 4.5 Response of concrete to uniaxial loading: (a) tension, (b) compression adapted from ABAQUS.

It can be seen in Fig. 4.5 that when strain softening occurs, the initial elastic stiffness is degraded. In another word, concrete is damaged. As presented in the figure, the moduli of damaged concrete under tension and compression can be estimated by $(1-d_t)E_0$ and $(1-d_c)E_0$, respectively. Note that E_0 is the initial (elastic) modulus of undamaged concrete while d_t and d_c are designated as damage variables for concrete under tension and compression, respectively; and both are less than 1.0. According to ABAQUS, the stress-strain relations for concrete under tension and compression are expressed in Equations 4.8

and 4.9, respectively. The parameters ε_t^{pl} and ε_c^{pl} are used to define the post failure behaviour of concrete. They are referred to as the equivalent tensile plastic strain and equivalent compressive plastic strain, and can be calculated using Equations 4.10 and 4.11. The parameter ε_t^{cr} represents the cracking strain of the undamaged concrete while ε_c^{in} stands for the crushing strain of the concrete.

$$\sigma_t = (1 - d_t) E_0 (\varepsilon_t - \varepsilon_t^{pl}) \quad (4.8)$$

$$\sigma_c = (1 - d_c) E_0 (\varepsilon_c - \varepsilon_c^{pl}) \quad (4.9)$$

$$\varepsilon_t^{pl} = \varepsilon_t^{cr} - \frac{d_t}{1 - d_t} \frac{\sigma_t}{E_0} \quad (4.10)$$

$$\varepsilon_c^{pl} = \varepsilon_c^{in} - \frac{d_c}{1 - d_c} \frac{\sigma_c}{E_0} \quad (4.11)$$

4.2.5 Interaction between concrete and steel bars

Maintaining the composite action, which is required to transfer loads between concrete and steel bars, has been numerically modeled. This load transfer mechanism is referred to as bond and can be idealized a continuous field of stress along the steel bars. In this study, the fully bonded interaction between concrete and steel bars has been considered. It should be mentioned that the fully bonded flexural and shear reinforcement detailing based on CSA23.3-14 supports this assumption.

4.2.6 Meshing

In this study, relatively dense meshes were defined near the beam supports where plastic hinges are expected to form in order to make the concrete and rebar meshes well

interacted. The contacts between longitudinal and transverse rebars were defined in such a way that penetration and sliding are prevented in two orthogonal directions. It should be noted that the steel bars were modeled as embedded and fully bonded elements within the concrete block at their cut-off points. Since the size of meshes is relatively sensitive in ABAQUS, sensitivity analyses were conducted in this study to select the most appropriate size for meshing. The selected mesh sizes of the beam elements ranged from 50 mm to 200 mm with an aspect ratio of less than 4.0 in the orthogonal directions. For the truss elements (for rebars), the maximum mesh size is 50 mm, and the meshes are distributed along the axial direction of the elements.

Figure 4.6 shows the five cases for the sensitivity analysis on meshing. The beam considered is the ductile one for the building located in Vancouver (i.e., beam D5, Table 3.3, Chapter 3). For this purpose, a two-span frame was considered. It should be mentioned that a similar configuration was also used by other researchers to investigate structural response due to column removal (e.g., Bao et al. 2015, Sasani and kropelnicki 2008, etc.). In particular, the mesh of the concrete beam contains 56 elements in the beam's cross-section, i.e. 7 elements along height and 8 elements along the width. Efforts have been made to use smaller mesh in the expected plastic hinge zone (i.e., end of the beams) where relatively heavy transverse reinforcement is required for ductile and moderately-ductile beams according to NBCC (2010). More specifically, the numbers of elements considered in the plastic zone are 5, 8, 11, 22, and 33 for Cases 1 to 5, respectively. The numbers of beam's mesh elements at the side of the missing column are selected to be the same as that in the plastic hinge zone in order to achieve symmetrical meshing about the middle span of the beam. Accordingly, the divisions for the remaining parts of the beam are 13, 16, 26,

52, and 26 for Cases 1 to 5, respectively. In addition, the preliminary results showed that meshing of the region outside the plastic hinge zone did not have significant effects on the beam response.

During the analysis, a vertical (downward) load was applied at the location of the removed column. This load was gradually increased; in the meantime the displacement at the location of load applied was monitored until the beam(s) failed. Note that the amplitude of the load itself was not important in the analysis. The bending moment at the left face of the column and the vertical displacement of the beam at the place where the load was applied were recorded, and the results are illustrated in Fig. 4.7. Please note that the displacement in Fig. 4.7 is normalized with respect to the beam span length (6.0 m). The results in the figure clearly show that the responses provided by Cases 3, 4, and 5 are almost the same while the response given by Case 1 is the smallest among the five cases considered. The response provided by Case 2 might be considered as an average. Given this, the size of meshing defined in Case 3 was selected for further analyses due to the significantly reduced computation time compared to Cases 4 and 5.

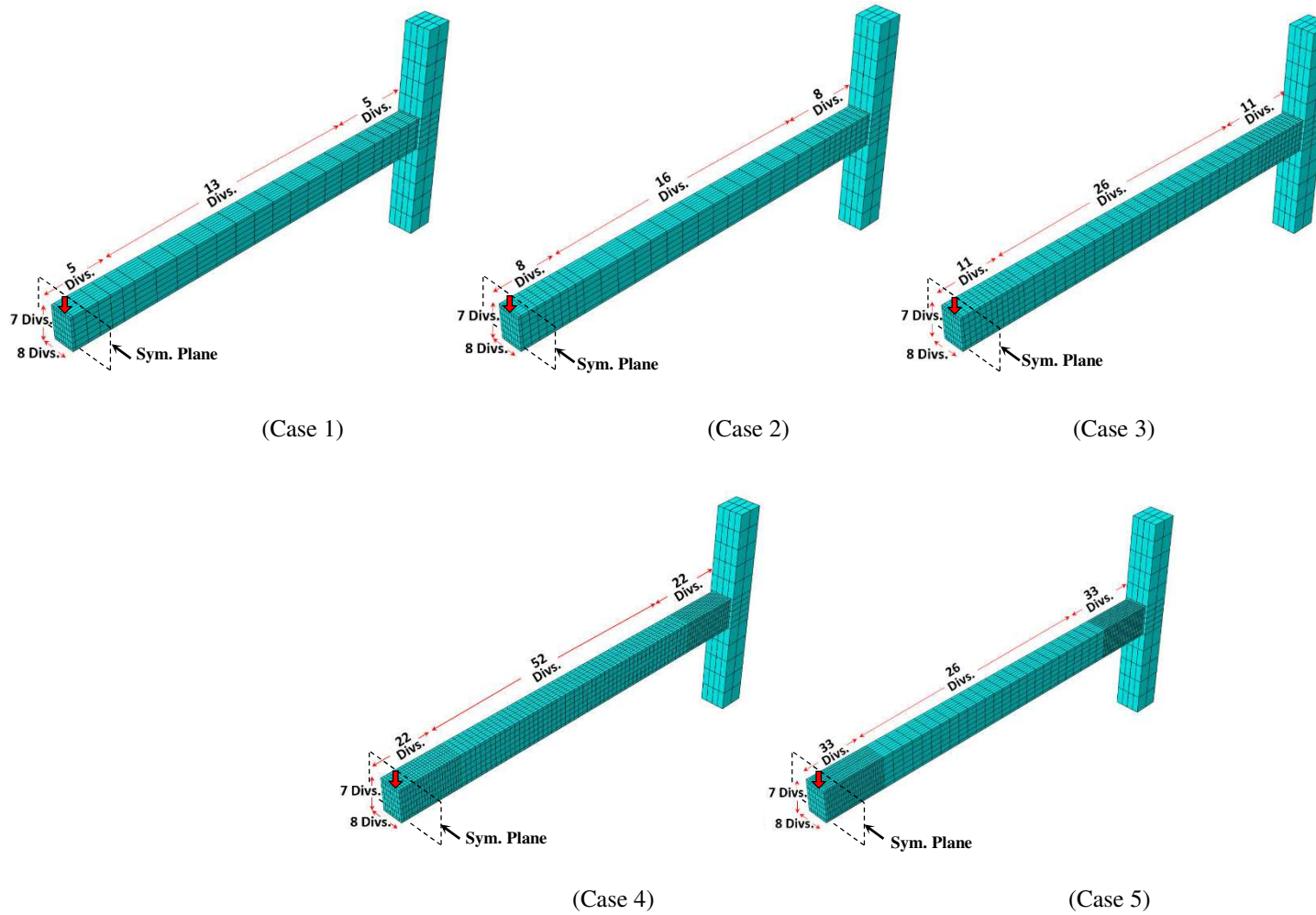


Figure 4.6 Cases for the sensitivity analysis on meshing.
 (Note: only part of the assembly is shown, the full assembly is given in Fig. 4.2)

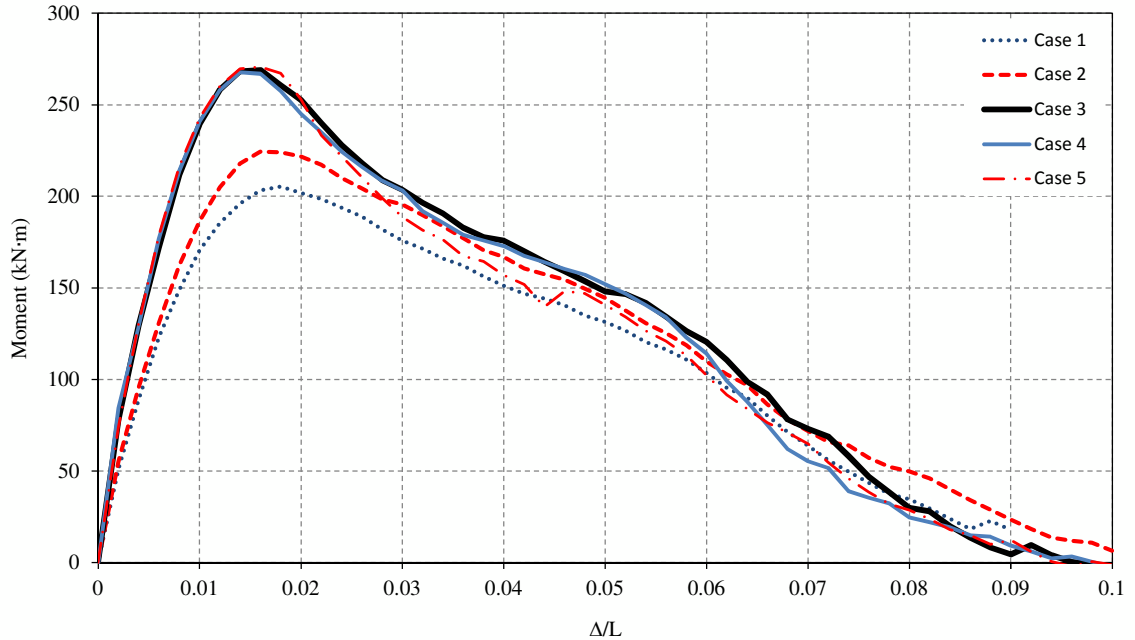


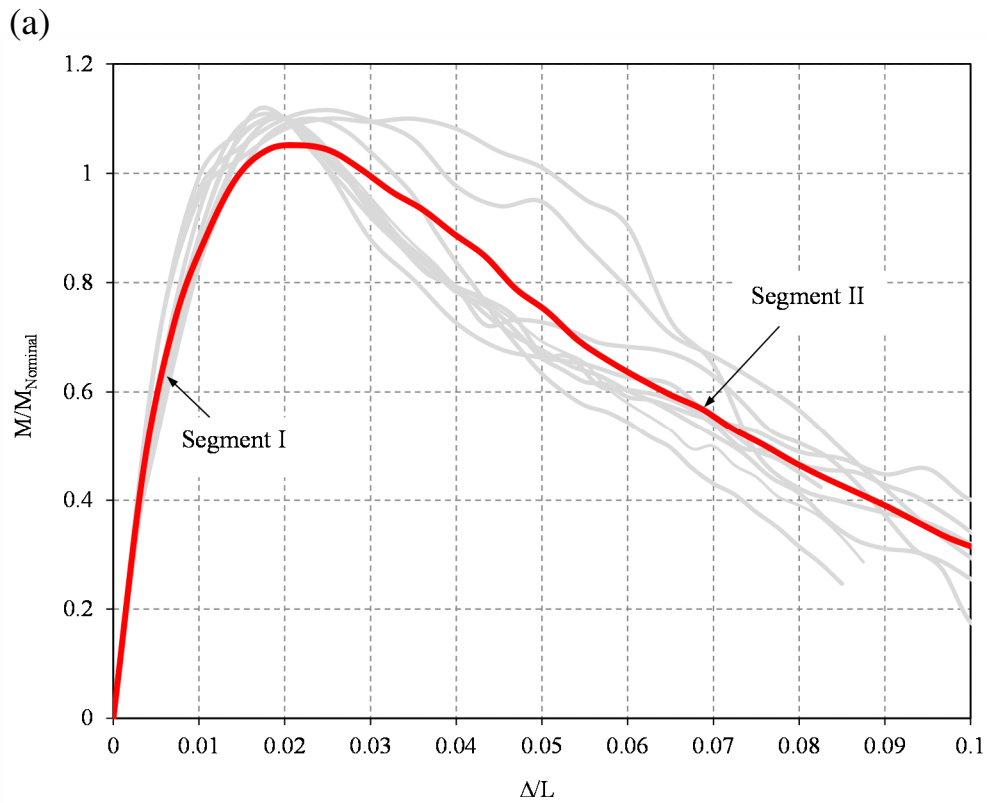
Figure 4.7 Beam responses from the sensitivity analyses.

4.3 Analysis results

4.3.1 Response curves

Following the techniques explained in the previous section, a comprehensive 3D finite element model was developed for each beam designed as described in Chapter 3. Nonlinear pushdown analysis was conducted on each model following the loading procedure described above. In general, the maximum displacement when the examined beams failed was about 10% of the span length. However, for some of the beams, the ratio dropped to about 8.5% due to the severe damage to the beam and/or convergence issues in ABAQUS. Figures 4.8a to 4.8c show the moment at the fixed end of the beam *vs.* the vertical displacement of the ductile (Vancouver buildings), moderately-ductile (Montreal buildings), and conventional beams (Toronto buildings), respectively, at the location where the column was removed. Each grey curve represents the response of each of nine beams

in the three studied seismicity locations; the red line presents the mean response curve. For purpose of comparison, the bending moment is normalized to the nominal moment resistance of the section while the displacement is normalized to the span length. It is worth mentioning that the mean response is not in the middle of the response curves, which can be seen clearly in Fig. 4.8a. This is because the mean values of the moments have been calculated using the associated moments at the same displacements. More specifically, the peak value of each curve is not happening in the same displacement as others, thus the mean curve is not located in the middle of the gray curves.



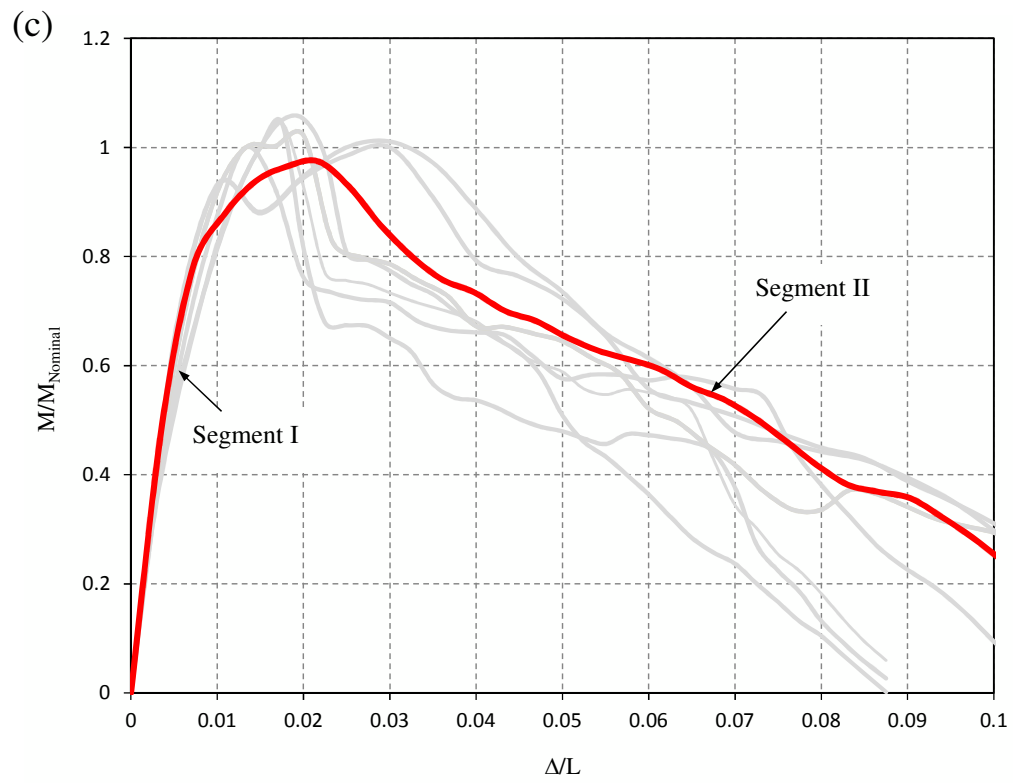
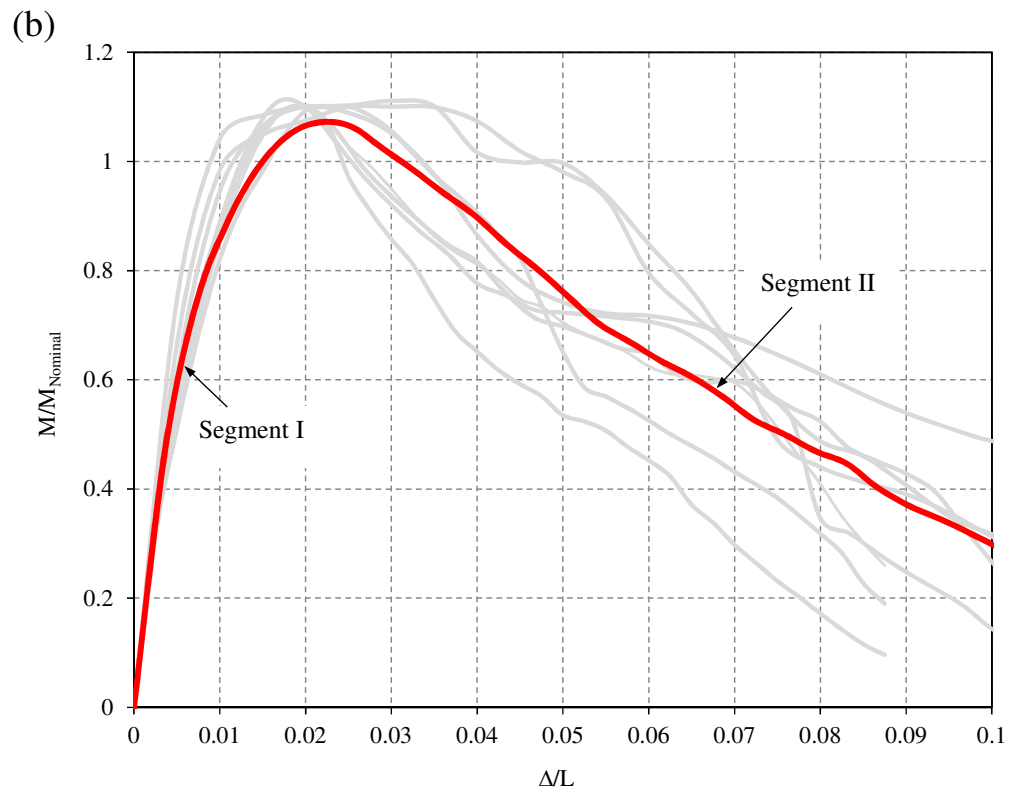


Figure 4.8 Beam response curves: (a) ductile beams, (b) moderately ductile beams, (c) conventional beam.

The results in Fig. 4.8 show that the response curve for ductile and moderately ductile beams is very similar, and they are different from that for conventional beams due to the different requirements for the seismic design (see Chapter 3). Moreover, the slope of the response curve for conventional beams for the displacement ratio Δ/L between 0.02 and 0.04 is relatively larger than that for ductile and moderately ductile beams for the same reason discussed above. It was also found that the slope of the curve beyond a Δ/L of 0.04 for the three types of beams is quite close. This is because they all lost their capacity when the displacement ratio Δ/L reached 0.04.

In fact, the response curves presented in Fig. 4.8 can be divided into three segments as follows,

- Segment I: represented by the curve up to the peak point in Fig. 4.8. The mechanism of the beam consists of cracking of concrete in tension and yielding of the longitudinal tensile reinforcement. This phase is controlled by flexural and compression membrane action.
- Segment II: used to represent the concrete crushing and the axial compressive force deformation (P- Δ) effect in beam section.
- Segment III (not shown in Fig. 4.8): the capacity of concrete is lost and the vertical load capacity of the beam increases due to catenary action (i.e., tension membrane action). As reported in Orton (2007), this phase usually appears when the vertical displacement of the beam reaches about 7.5% to 10% of the span length. Furthermore, due to the catenary action, the response might reach up to the value of the first peak shown in Segment I.

4.3.2 Development of parameters for modelling plastic hinges in beams

As discussed above, behaviour of the three types of beams against progressive collapse due to the column removal is different. Figures 4.9a and 4.9b illustrate the curves proposed in this study to model the plastic hinges in the ductile/moderately ductile and conventional beams, respectively. The red curves in the figures are adapted from those in Fig. 4.8, in which the horizontal axis is converted to the rotation from the normalized displacement ratio Δ/L . More specifically, the rotation was calculated by using the vertical displacement of each beam at the location of 12% of span length divided by the corresponding horizontal displacement of the point in the beam assessed. It has been observed that the points located in the distance between the column face and 12% of span length rotate equally.

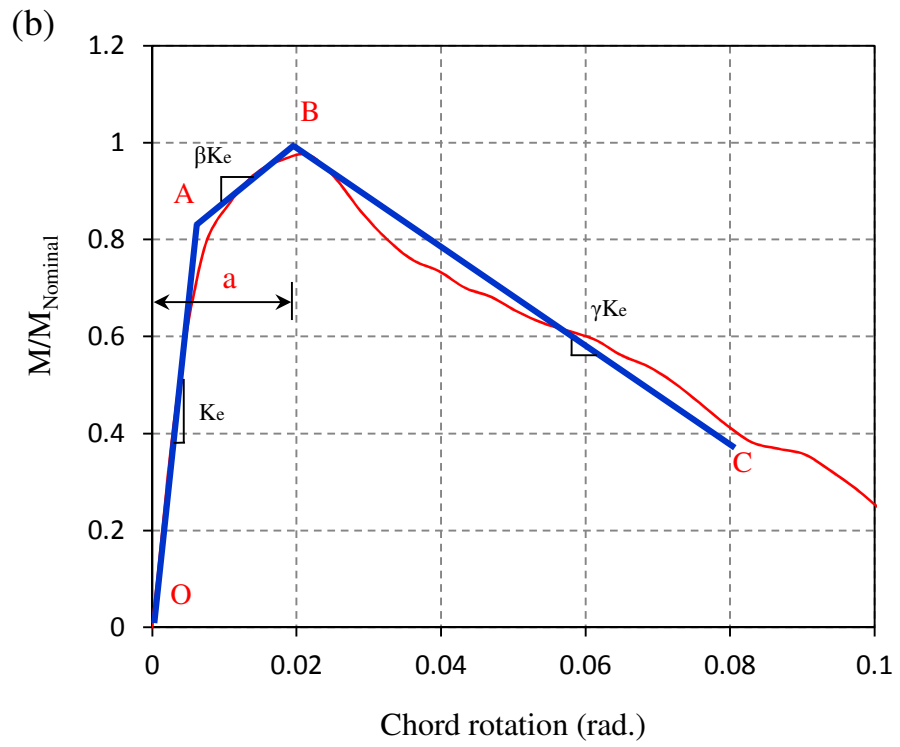
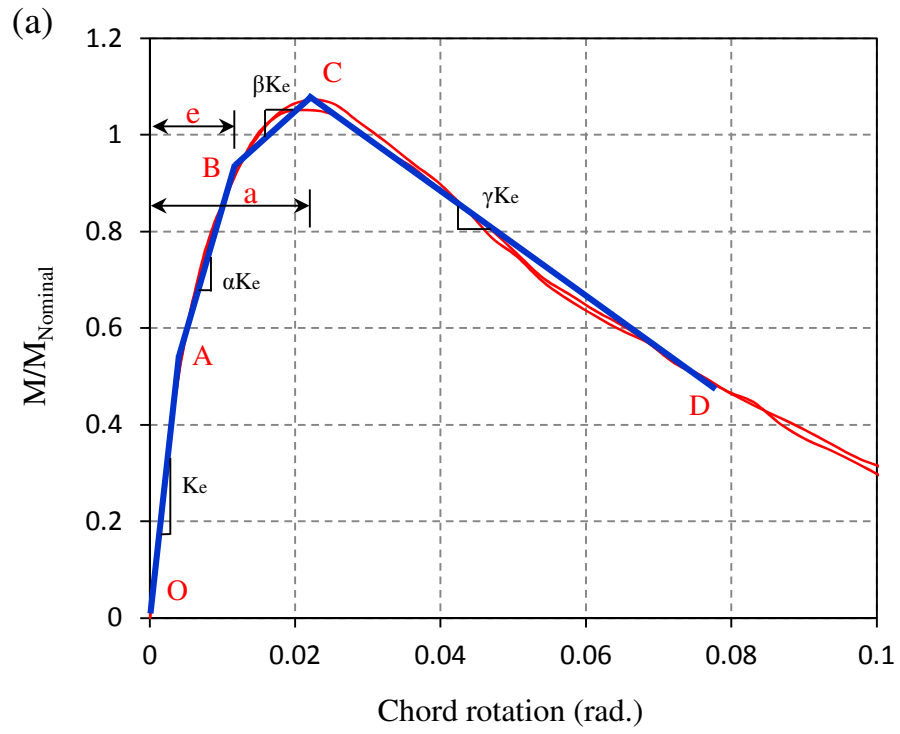


Figure 4.9 Multi-linear backbone curve for modeling plastic hinges in beam:
 (a) ductile and moderately ductile beams, (b) conventional beams

As seen in Fig. 4.9, the same multi-linear curve was proposed for the ductile and moderately ductile beams since their mean response curve is very close (Figs. 4.8a and 4.8b), while a tri-linear curve was developed for the conventional beams. The mean values for the typical points on the response curves illustrated in Fig. 4.9 are provided in Table 4.1. A detailed description of each curve is given below.

- For **ductile/moderately ductile beams** (Fig. 4.9a): point **A** is used to represent the first yield in the longitudinal steel bars, which corresponds to about 50% of the nominal capacity of the section; point **B** stands for the nominal bending moment capacity of the beam; point **C** represents the ultimate capacity, which is about 10% higher than the nominal capacity; and point **D** represents the failure of the section.
- For **conventional beams** (Fig. 4.9b): point **A** is used to represent the first yield in the longitudinal steel bars, which corresponds to about 80% of the nominal capacity of the section; point **B** stands for the nominal bending moment capacity of the beam; and point **C** represents the failure of the section.
- The slope of every two adjacent points on the proposed curve is defined with respect to the initial elastic stiffness K_e using parameters α , β , and γ .

Table 4.1 Mean values for the modelling parameters proposed.

	Parameters	Ductile and moderately ductile	Conventional
Tangents	α	0.26	N.D.
	β	0.45	0.1
	γ	-0.075	-0.08
Coordinates	A	(0.003,0.5)	(0.006,0.8)
	B	(0.0145,1)	(0.02,1)
	C	(0.025,1.1)	(0.08,0.32)
	D	(0.08,0.4)	N.D.

4.3.3 Prediction of the modelling parameters

Instead of using the mean values to define the typical points on the response curves, such as Points B and C in Fig. 4.9a, formulations of the typical model parameters a' and e' for the ductile (moderately ductile) and conventional beams were developed using Minitab17, and they are expressed as follows,

$$a' = \frac{L \cdot R_d}{81 - L(0.06 + 7R_d - 69\eta)} \quad (4.12)$$

$$e' = \frac{L \cdot R_d}{316 - L(40 + 10R_d - 21\eta)} \quad (4.13)$$

The parameter a' is used to represent the expected chord rotation of beam when the ultimate bending moment capacity of the beam is reached, i.e., the rotation of point C in Fig. 4.9a and that of point B in Fig. 4.9b. The parameter e' represents the chord rotation corresponding to the nominal bending moment capacity for conventional/moderately ductile beams, i.e., the rotation of point B in Fig. 4.9a. Please note that this parameter is not required to define the modeling parameters for conventional beams. In the two

equations proposed, L represents the span length of the beam, in m; R_d is the ductility-related factor for the seismic design of the frames (for conventional beams, $R_d = 1.5$; for moderately ductile beams, $R_d = 2.5$; for ductile beams, $R_d = 4.0$); $\eta = \frac{\rho - \rho'}{\rho_b}$, in which ρ and ρ' are reinforcement ratios for tension reinforcement and compression reinforcement, respectively; and ρ_b is the reinforcement ratio for a balanced section.

It is worth mentioning that Equations 4.12 and 4.13 were developed based on the results from all of the 27 cases (i.e., beams) under investigation. More specifically, the response curve of each beam shown in Fig. 4.8 was idealized as a multi-linear curve (for ductile and moderately ductile beams) or tri-linear curve (for conventional beams) following the approach to idealize the mean response curves shown in Fig. 4.9. In total, 27 and 18 data points for parameters a and e were defined respectively, in which each point is associated with three variables, i.e., L , R_d , and η . Gauss–Newton algorithm was chosen to fit each of the two parameters a and e with the variables mentioned above. The mean squared errors of the proposed functions for a' and e' were about 0.0014 and 0.0057, respectively. Furthermore, it was found that the maximum residual, which represents the difference between the value of the parameter (a' and e') predicted using the proposed equation and the actual value, was about 0.07. For the purpose of comparison, Figure 4.10 shows the values for the parameter a and GSA 2013 for the 27 cases considered in this study. It can be clearly seen that the GSA value is much larger (about 2 times larger in average values) than that from the detailed finite element analysis. It is worth mentioning herein that very close response to the proposed model was observed in the experimental

study conducted by Qian and Li (2013). The red circles shown in the Fig 4.10 represent the chord rotation of three similar beams considered in the study.

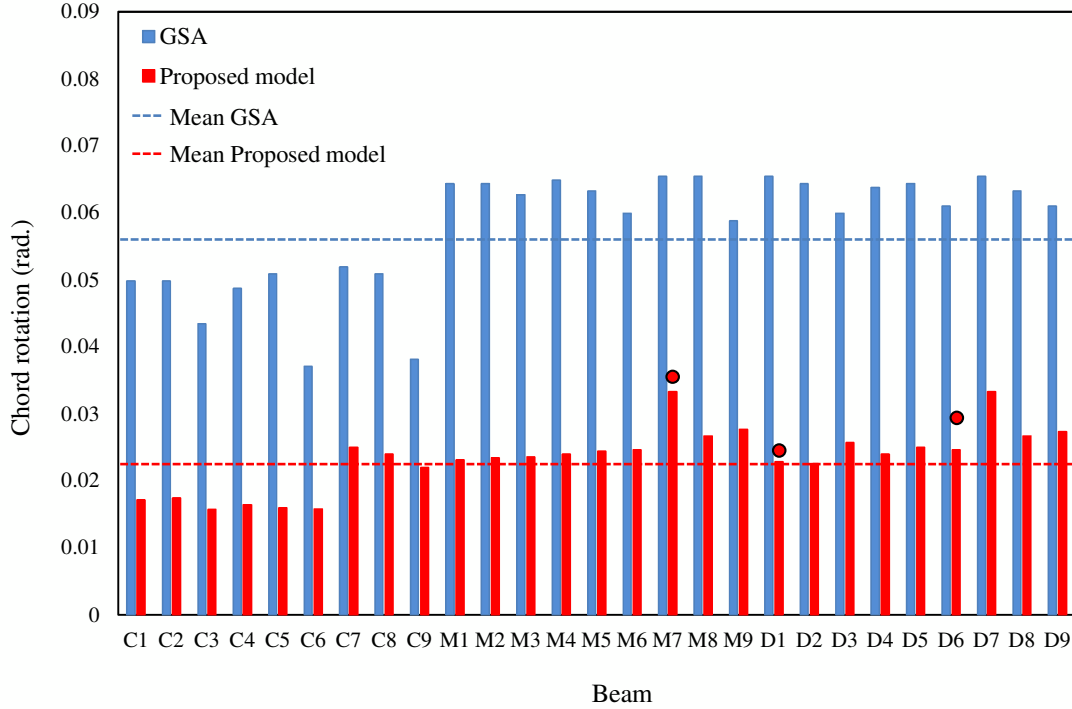


Figure 4.10 Comparison of the value for parameter a' based on the proposed model and 2013 GSA.

4.3.4 Comparison with the parameters proposed in 2013 GSA

Figures 4.11a, and 4.11b present the response curves proposed in this study with the superposition of those specified in 2013 GSA for ductile/moderately ductile, and convention RC beams, respectively. The shaded area and the red lines in the figure are used to represent the range of the response curve enclosed by the lower and upper bounds of the parameters defined in GSA and the proposed model. For the purpose of comparison, the red dashed lines show the lower and upper bounds of the proposed model. The major differences observed are summarized as follows,

- According to the 2013 GSA definition, the maximum bending moment capacity of beams is always equal to the nominal capacity of the section regardless of the level of the ductility. By comparison with the curves proposed in this study, it can be seen that the bending moment capacity of the ductile/moderately ductile beams is underestimated in the 2013 GSA.
- The stiffness of the post peak (ultimate) response curve remains constant in 2013 GSA. However, detailed finite element analysis results in this study show that the change of the stiffness depends on the level of the plasticity in the beam.
- The post yield and failure mechanism of the beams are observed to follow a relatively small slope to descend (i.e., 0.075 for ductile/moderately ductile, and 0.08 for conventional). However, 2013 GSA defines a sudden drop on the response once the full capacity is reached.

4.4 Summary

For the purpose of this study, 27 finite element models for beams were developed using ABAQUS. The material properties of steel reinforcement and concrete were defined and the concrete damage plasticity method was used in order to represent the nonlinear behaviour of concrete. The responses of bending moment vs. the displacement of the beams, during the push down analysis were recorded. Two equations were proposed to determine the modeling parameters of the beams to include the span length, level of ductility (i.e., ductile, moderately ductile and conventional) and longitudinal reinforcement ratio. At the end, the proposed modeling parameters were compared to those recommended by 2013 GSA.

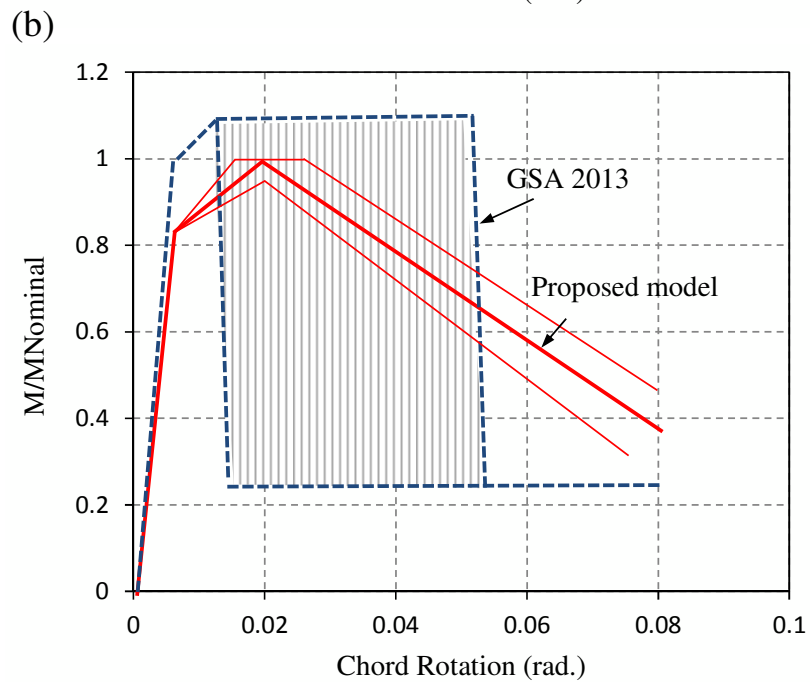
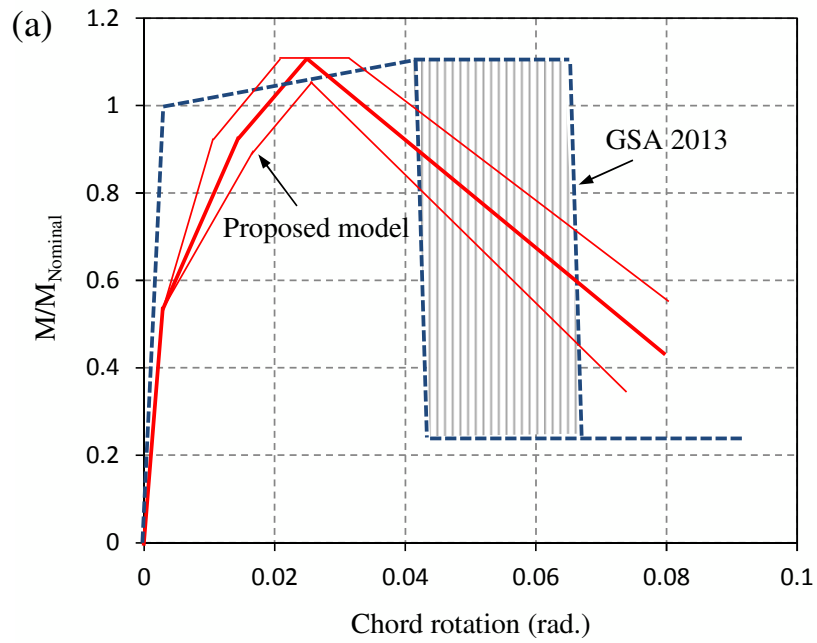


Figure 4.11 Comparison of the proposed model with 2013 GSA criteria:
 (a) ductile/moderately ductile beams, (b) conventional beams.

Chapter 5

CONCLUSIONS AND RECOMMENDATIONS

5.1 Introduction

The objective of this study is to assess the bending moment capacity of RC beams and define the modeling parameters for lumped plastic hinges for the progressive collapse analysis. Given this, 27 RC buildings were designed based on the recent version of CSA standard for the design of concrete structures and the 2010 edition of the National Building Code of Canada. The buildings are designed as conventional, moderately-ductile, and ductile as part of seismic moment-resisting frames located in Toronto (low seismicity), Montreal (medium seismicity), and Vancouver (high seismicity), respectively. The span lengths of the beams are 4.0, 6.0 and 8.0 m, which are used to represent the typical spans for the RC buildings. Three-dimensional finite element models were developed using ABAQUS to investigate the behavior of the beam-column assembly due to the removal of the column supporting the beam. Nonlinear pushdown analysis was conducted in order to capture the nonlinearity of the materials (i.e., concrete and reinforcing steel) and geometry of the beam elements. The bending moment – chord rotation relationship for each beam was recorded. Based on the analysis results, backbone moment-rotation curves for the conventional, and ductile/moderately-ductile beams were developed, respectively. In addition, two equations were proposed to predict the rotations corresponding to the maximum moment capacity and the moment capacity for the first yielding of the steel bars. They can be used to define the moment-rotation curve for RC beams for a given span

length, reinforcement ratio, and ductility. Furthermore, the curves proposed in the study were compared with those given in 2013 GSA.

5.2 Conclusions

The main conclusions of this study are summarized as follows:

- The level of seismic design ductility level of the RC buildings significantly affects its progressive collapse resistance. It was found that the bending moment capacity of the studied beams with seismic detailings was about 10% larger than the nominal capacity. However, the capacity of the conventional beams did not exceed its nominal value.
- The shapes of the moment-rotation curve for the ductile and moderately ductile RC beams is very similar, but are different than that for the conventional beams. Based on the analyses of the 27 cases for the beam-column assembly, it was observed that the nonlinear behaviour of the ductile and moderately ductile beams could be represented by a multilinear curve. It consists of four segments that represent the beam capacity corresponding to the first yielding of the steel bar, 80% of its nominal capacity, ultimate capacity, and failure of the beam, respectively. This is different than the cyclic behaviour of conventional beams that is typically modeled by a trilinear curve with three branches that represent the beam yield capacity, nominal capacity, and failure. The post-yield stiffnesses of the ductile/moderately ductile and conventional beam are about 26% and 45% of the initial elastic stiffness.

- In comparison with the 2013 GSA modeling parameters, smaller chord rotations (about 50% less) were estimated from the detailed finite element analysis.
- The allowable rotation in RC beams, which is used in assessing the progressive collapse resistance, depends on the rotation at the ultimate bending moment. Detailed characterization of the beam behaviour after the peak capacity may not be needed because significant loss of the strength was observed in the analysis, which could lead to the immediate collapse of the element. This statement is valid unless the second peak is reached due to the effect of catenary action.
- The length of the RC beams' plastic hinge was found to be approximately about 1.5 times the overall thickness of the beam, which is consistent with that specified in the seismic design provisions of CSA A23.3-14. Furthermore, seismic detailings were found to be efficient on preventing shear failure of the beams, i.e., flexural failure of the ductile and moderately ductile beams were observed.
- The proposed equations in Chapter 4 can be used for nonlinear modeling of plastic hinges in RC beams (i.e., characterizing the lumped plastic hinges in macro modeling). These equations include the effects of the beam's geometry, reinforcements and levels of ductility.

5.3 Recommendations for future research

The research work presented in this thesis is based on investigation the response of a beam-column assembly of RC moment-resisting frame buildings due to the removal of a column at the center of the structure. This represents a portion of possible cases for progressive collapse analysis of buildings. Given this, further research is needed as summarised hereafter:

- Effects of vertical structural members (e.g., columns and shear walls) on the behaviour of beams because the interaction between beam and column might affect the response of beams.
- Behaviour of other types of beams, e.g., deep beams, beams under significant shear forces, also need to be investigated.
- Detailed modeling of beam-column joints in RC buildings should be considered in the progressive collapse analysis in order to evaluate the effect of failure of joints on beam response.
- Contribution of the concrete slab to the progressive collapse resistance including the effects of the slab integrity reinforcement joints on beam response.
- Considering the debonding of the reinforcement and concrete, especially in post peak behaviour might lead to more realistic results.

APPENDIX A

Design of Reinforcement for Beams

A.1 Design of flexure reinforcement

The bending moment capacity of the beam is calculated in accordance with CSA standard A23.3-04 (CSA 2014). It should be noted that strain hardening of the reinforcing steel and the confinement effects are not considered in the calculations. Figure A.1 illustrates the plane section method that uses the compatibility condition.

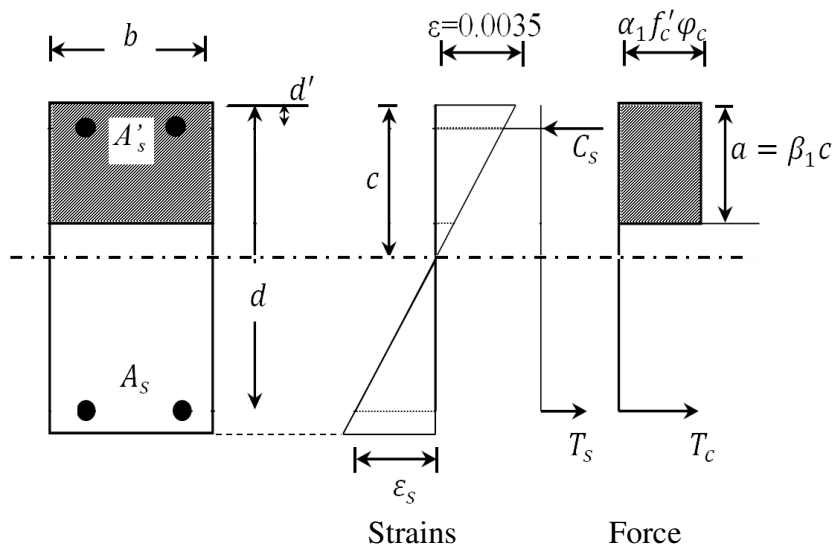


Figure A.1 Plane section method.

A.1.1 Design singly reinforced sections

- The depth of the equivalent concrete stress block, a , can be determined using Eq. A.1,

$$a = d - \sqrt{d^2 - \frac{2M_f}{\alpha_1 \phi_c f'_c b}} \quad (\text{A.1})$$

Where,

d = distance from extreme compression fiber to centroid of longitudinal tension reinforcement,

b = width of the section,

M_f = factored moment,

ϕ_c = Resistance factor for concrete, taken as 0.65,

f'_c = compressive strength of concrete, taken as 40 MPa in this study,

$\alpha_1 = 0.85 - 0.0015 f'_c \geq 0.67$ (CSA 10.1.7).

- The depth of the equivalent concrete stress block for a balanced condition, a_b , can be calculated using Eq. A.2,

$$a_b = \beta_1 c_b \quad (\text{A.2})$$

Where,

$\beta_1 = 0.97 - 0.0025 f'_c \geq 0.67$ (CSA 10.1.7),

$$c_b = \frac{700}{700 + f_y} d,$$

f_y = Yield strength of reinforcing steel, taken as 200000 MPa in this study.

- If $a < a_b$, the area of the reinforcement in tension is computed by Eq. A.3 in which ϕ_s represents the resistance factor for reinforcing bars, and it is taken as 0.85 in this study. The tensile reinforcement should be placed at the bottom of the section if the design moment is positive or at the top if the moment is negative.

$$A_s = \frac{M_f}{\phi_s f_y \left(d - \frac{a}{2} \right)} \quad (\text{A.3})$$

- If $a > a_b$, then the compression reinforcement should be provided, i.e., the section should be designed as a doubly reinforced section following the procedure described in the section below.

A.1.2 Design doubly reinforced sections

The total area of the steel bars under compression can be calculated as follows,

Step 1: Determine the factored moment resistance of a balanced section tension, M_{fb} , using

Eq. A.4,

$$M_{fb} = C \left(d - \frac{a_b}{2} \right) \quad (\text{A.4})$$

Where C is the factored compressive force developed in concrete, which can be determined using Eq. A.5

$$C = \alpha_1 \phi_c f'_c b a_b \quad (\text{A.5})$$

Step 2: Determine the area for the compression steel (A'_s) using Eq.

$$A'_s = \frac{M_f - M_{fb}}{(\phi_s f'_s - \alpha_1 \phi_c f'_c)(d - d')} \quad (\text{A.6})$$

Where,

d' = distance from extreme compression fiber to centroid of compression reinforcement,

f'_s = strength of the compression reinforcement, and can be calculated using Eq. A.7,

$$f'_s = 0.0035E_s \left(\frac{c-d'}{c} \right) \leq f_y \quad (\text{A.7})$$

Step 3: Determine the area for the tension steel (A_s) using Eq. A.8,

$$A_s = \frac{M_{fb}}{\phi_s f_y \left(d - \frac{a_b}{2} \right)} + \frac{M_{fb}}{\phi_s f_y (d - d')} \quad (\text{A.8})$$

A.1.3 Minimum and maximum reinforcement

The minimum tensile reinforcement required for a beam section, $A_{s,min}$, shall be determined according to Clause CSA 10.5.1.2 in which b_t represents the width of the tension zone of the section (Eq. A.9); the maximum reinforcement ratio is limited to 4%.

$$A_{s,min} = \frac{0.2\sqrt{f'_c}}{f_y} b_t h \quad (\text{A.9})$$

A.2 Design of shear reinforcement

Shear design of buildings due to seismic loads is different than those without seismic loads as stipulated in CSA A23.3-04. More specifically, the design of shear forces, V_f for ductile moment-resisting frames (e.g., frames of buildings in Vancouver) and moderately-ductile moment-resisting frames (e.g., frames of buildings in Montreal) should be determined based on the probable moment resistance and nominal moment resistance, respectively, in addition to the shear due to the gravity loads. However, the design shear strength might not be taken greater than the factored shear force with the seismic load

amplified by a factor of $R_d R_o$ in accordance with CSA Clauses 21.3.4 and 21.7.2. It is also necessary to mention that shear design of conventional moment-resisting frames (e.g., frames of buildings in Toronto) is the same as that of the frames without seismic loads.

- The factored concrete shear resistance can be calculated using Eq. A.10 according to CSA Clause 11.3.4

$$V_c = \phi_c \lambda \beta \sqrt{f'_c} b_w d_v \quad (\text{A.10})$$

Where,

λ = Factor for concrete density. For normal density concrete, it is taken as 1.0,

β = Factor accounting for shear resistance of the concrete (CSA 2.2). It should be noted that β is taken as zero for shear design of plastic hinge region for ductile moment-resisting frames.

b_w = Width of web. For rectangular beams, it is equal to the width of the beam.

d_v = Effective shear depth, taken as the greater of $0.9d$ or $0.72h$.

In order to determine the shear reinforcement, the following conditions must be checked,

- Condition I: If V_f is less than V_c , then no shear reinforcement is required.
- Condition II: if $V_f \leq V_c \leq V_{r,\max}$, then the shear reinforcement should be designed using Eq. A.11, in which A_v is the area of shear reinforcement with a distance s . In the equation, θ is the angle of inclination of compressive stress to the longitudinal axis of the member.

$$\frac{A_v}{s} = \frac{(V_f - V_c) \tan \theta}{\phi_s f_y d_v} \quad (\text{A.11})$$

- As specified in CSA, the minimum shear reinforcement should be provided in the following regions:

(1) Where the factored shear force V_f exceeds V_c ,

(2) Where the overall depth is greater than 750 mm, and

(3) In region where the factored torsion T_f exceeds 0.25.

- Where the minimum shear reinforcement is required, the minimum area of shear reinforcement should be computed using Eq. A. 12,

$$\frac{A_v}{s} \geq 0.06 \frac{\sqrt{f'_c}}{f_y} b_w \quad (\text{A.12})$$

A.3 Additional considerations for seismic design of beams

In addition to the requirements described above, additional considerations for the design of ductile and moderately-ductile moment-resisting frames required by CSA A23.3-04 are summarized as follows,

- The minimum longitudinal reinforcement on both the top and bottom of the beam should be larger than that given in Eq. A.13 (CSA Clause 21.3.2.1)

$$A_{s,\min} \geq \frac{1.4}{f_y} b_w d \quad (\text{A.13})$$

- At any support of the ductile beam, the positive moment resistance would not be less than one-half of the negative moment resistance. For moderately-ductile beam, the ratio is reduced to one third.
- Positive and negative moment resistance of any section along the span would not be less than one-fourth of the positive or negative moment resistance of the ductile beam end section; one-fifth for the moderately-ductile beam.
- For the shear design of ductile beams, the shear capacity of the beam should be checked for the probable shear due to the probable moment capacity and the factored gravity load. This is an additional shear check besides the one required for conventional beam. The shear capacity of the concrete should be neglected in ductile beams.
- In order to calculate the probable shear capacity of ductile beams, the overstrength factor is taken as 1.25 and $\phi_c = \phi_s = 1.0$.

A.4 Sample of design

As an example, detailed design of a ductile beam with the span length of 6.0 m is presented below.

The beam section is assumed to be 300 × 500. The preliminary dimension of the beam section is computed based on the Table 9.2 of CSA23.3-14 for the beams which are likely to be damaged by large deflections.

$$h \geq \frac{l_n}{21} = \frac{6000-500}{21} = 261.90 \rightarrow h = 500 \text{ mm}, b = 300 \text{ mm}$$

$$d = h - \text{cover} = 500 - 50 = 450 \text{ mm}$$

A.4.1 Flexure design

$$\alpha_1 = 0.85 - 0.0015f'_c \geq 0.67 \rightarrow \alpha_1 = 0.85 - 0.0015(40) = 0.79$$

$$\beta_1 = 0.97 - 0.0025f'_c \geq 0.67 \rightarrow \beta_1 = 0.97 - 0.0025(40) = 0.87$$

$$c_b = \frac{700}{700 + f_y} d \rightarrow c_b = \frac{700}{700 + 400} (450) = 286.36 \text{ mm}$$

$$a_b = \beta_1 c_b \rightarrow a_b = 0.87 * 286.36 = 249.13 \text{ mm}$$

For the negative bending moment @ support: $M_r \geq M_f = 148.2 \text{ kN} \cdot \text{m}$

$$a = d - \sqrt{d^2 - \frac{2M_f}{\alpha_1 \phi_s f'_c b}} \rightarrow a = 450 - \sqrt{450^2 - \frac{2 * 148.2 * 10^6}{0.79 * 0.65 * 40 * 300}} = 57.06 \text{ mm} < a_b$$

$$A_s = \frac{M_f}{\phi_s f_y \left(d - \frac{a}{2} \right)} \rightarrow A_s = \frac{148.2 * 10^6}{0.85 * 400 \left(450 - \frac{57.06}{2} \right)} = 1034.19 \text{ mm}^2 \rightarrow$$

Use: 2 – 20M + 1 – M25 (Top) → Area = 1100 mm²

For the positive bending moment @ midspan: $M_r \geq M_f = 77.69 \text{ kN} \cdot \text{m}$

$$a = d - \sqrt{d^2 - \frac{2M_f}{\alpha_1 \phi_c f'_c b}} \rightarrow a = 450 - \sqrt{450^2 - \frac{2 \cdot 77.69 \cdot 10^6}{0.79 \cdot 0.65 \cdot 40 \cdot 300}} = 28.95 \text{ mm} < a_b$$

$$A_s = \frac{M_f}{\phi_s f_y \left(d - \frac{a}{2}\right)} \rightarrow A_s = \frac{77.69 \cdot 10^6}{0.85 \cdot 400 \left(450 - \frac{28.95}{2}\right)} = 524.65 \text{ mm}^2 \rightarrow$$

Use: 2 – 20M (Bottom) → Area = 600 mm²

$$A_{s,\min} = \frac{0.2 \sqrt{f'_c}}{f_y} b_t h \rightarrow A_{s,\min} = \frac{0.2 \cdot \sqrt{40}}{400} * 300 * 450 = 426.90 \text{ mm}^2$$

$$A_{s,\max} = 0.04 * 300 * 450 = 5400 \text{ mm}^2$$

A.4.2 Shear design

For the shear @ support: $V_f = 100.45$

$$V_c = \phi_c \lambda \beta \sqrt{f'_c} b_w d_v \rightarrow V_c = 0.65 * 1.0 * 0.163 * \sqrt{40} * 300 * 405 = 81.41 \text{ kN}$$

$$d_v = \max(0.9d, 0.72h) = \max(405, 360) = 405$$

$$\beta = \frac{230}{1000 + d_v} = \frac{230}{1000 + 405} = 0.163$$

$$\frac{A_v}{s} = \frac{(V_f - V_c) \tan \theta}{\phi_s f_y d_v} \rightarrow \frac{A_v}{s} = \frac{(100.45 - 81.41) \cdot 1000 \cdot \tan(35)}{0.85 \cdot 400 \cdot 405} = 0.0815$$

Use 10M @ 220mm

$$\frac{A_v}{s} \geq 0.06 \frac{\sqrt{f'_c}}{f_y} b_w \rightarrow \frac{A_v}{s} \geq 0.06 * \frac{\sqrt{40}}{400} * 300 = 0.284$$

A.4.3 Additional consideration for seismic design

- Flexure Design:

$$A_{s,min} \geq \frac{1.4}{f_y} b_w d \rightarrow A_{s,min} \geq \frac{1.4}{400} * 300 * 450 = 472.5 \text{ mm}^2$$

$$\rho \leq 0.04, \rho \geq \frac{0.2 \sqrt{f'_c}}{f_y} = 0.0031$$

$$M_{u \text{ Support}}^+ \geq \frac{1}{2} M_{u \text{ Support}}^- \rightarrow M_{u \text{ Support}}^+ \geq \frac{148.2}{2} = 74.1 \text{ kN.m} \rightarrow A_s = 517.1 \text{ mm}^2$$

Use: 2 – 20M (Bottom) → Area = 600 mm²

$$M_{u \text{ mid-span}}^+ \geq \frac{1}{4} \max\{M_{u \text{ Support}}^-, M_{u \text{ Support}}^+\} \rightarrow M_{u \text{ mid-span}}^+ \geq \frac{1}{4} 148.2 = 37.05$$
$$\rightarrow A_s = 258.5 \text{ mm}^2 \leq 600 \text{ mm}^2$$

$$M_{u \text{ mid-span}}^- \geq \frac{1}{4} \max\{M_{u \text{ Support}}^-, M_{u \text{ Support}}^+\} \rightarrow M_{u \text{ mid-span}}^- \geq \frac{1}{4} 148.2 = 37.05$$
$$\rightarrow A_s = 258.5 \text{ mm}^2$$

Use: 1 – 25M (Top) → Area = 600 mm²

- Shear Design:

$$V_f = V_P + V_{D+L}$$

V_p = Shear force obtained by applying the calculated probable ultimate moment capacities.

L_n is the net span length.

$$V_p = \frac{M_i^- + M_j^+}{L_n} = \frac{232.12 + 107.15}{5.5} = 60.4 \text{ kN}$$

$$V_f = 60.4 + 73.39 = 133.79$$

$$\frac{A_v}{s} = \frac{V_f \tan \theta}{\phi_s f_y d_v} \rightarrow \frac{A_v}{s} = \frac{(133.79) * 1000 * \tan(35)}{0.85 * 400 * 405} = 0.68$$

Use 10M @ 100mm in distance of 1150 mm from column face, and 10M @ 200mm in the rest area.

REFERENCES

ABAQUS 6.11. 2011. Analysis User's Manual. Simulia.

ACI. 2011. ACI Committee. Building code requirements for structural concrete and commentary (318-11), Washington, D.C.

Ahmed, A. 2014. Modeling of a reinforced concrete beam subjected to impact vibration using ABAQUS. International Journal Of Civil And Structural Engineering. Vol. 4, Issue 3, 227-236.

ASCE/SEI 41-13. 2014. Seismic evaluation and retrofit of existing building. American Society of Civil Engineers, Reston, VA.

Astaneh-Asl, A. 2001. Progressive collapse resistance of steel building floors. American Institute of Steel Construction. UCB/CEE-Steel-2001/03.

Astbury, N. F. 1969. Brickwork and gas explosions. The British Ceramic Research Association. Technical note No. 146.

Bennett, R. M. 1988. Formulations for probability of progressive Collapse. Structural Safety. Vol. 5, Issue 1, 67-77.

Breen, J. E. 1975. Progressive collapse of building structures. Workshop held at the University of Texas at Austin, Austin, TX.

Burnett, E. F. P. 1974. Abnormal loadings and the safety of buildings. Center for Building Technology. Institute for Applied Technology, National Bureau of Standards, Washington, D.C.

Burnett, E. F.P. 1973. residential buildings and gas-related explosions. Center for Building Technology. Institute for Applied Technology, National Bureau of Standards, Washington, D.C.

Casciati, F., and Faravelli, L. 1984. Progressive failure for seismic reliability analysis. *Engineering Structures*, Vol. 6, Issue 2, 97-103.

CEB-FIP. 1991. Comité Euro-International du Béton. Thomas Telford, Lausanne, Switzerland.

CSA. 2014. Design of concrete structures. Standard CAN/CSA-A23.3-14, Canadian Standard Association, Mississauga, Ont.

Deng, S., Qie, Z., and Wang, L. 2015. Nonlinear analysis of reinforced concrete Beam bending failure experimentation based on ABAQUS. First International Conference on Information Sciences, Machinery, Materials and Energy, ISSN: 1951-6851.

Dusenberry, D. O. 2002. Review of existing guidelines and provisions related to progressive collapse. Workshop on Prevention of Progressive Collapse, National Institute of Building Sciences (NIST), Rosemont, IL.

FEMA 403. 2002. World trade center building performance study. Federal Emergency Management Agency, New York.

Ferahian, R. H. 1971. Design against progressive collapse. National Research Council of Canada, Division of Building Research, Ottawa, Ont.

Grierson, D. E., Safi, M., Xu, L., and Liu, Y. 2005. Simplified methods for progressive-collapse analysis of buildings. Proceedings of ASCE 2005 Structures Congress. New York, NY. pp.8.

Gross, J. L., and McGuire, W., 1983. Progressive Collapse Resistant Design. *Journal of Structural Engineering*, Vol. 109, Issue 1, 1-15.

GSA. 2003. Progressive collapse analysis and design guidelines for new federal office buildings and major modernization projects. U.S. General Service Administration, Washington, D.C.

GSA. 2013. Alternate path analysis and design guidelines for progressive collapse resistance. U.S. General Service Administration, Washington, D.C.

- Heger, F. J. 2006. L'Ambiance Piazza. Retrieved from (www.engineering.com).
- IBC. 2015. International Building Code. International Code Council (INC.), Country Club Hills, IL.
- ISC. 2013. The Risk Management Process for Federal Facilities. Interagency Security Committee Standard, Washington, D.C.
- Izzuddin, B. A., Vlassis, A. G., Elghazouli, A. Y., Nethercot, D. A., 2008. Progressive collapse of multi-storey buildings due to sudden column loss - Part I: Simplified assessment framework. *Journal of the Institution of Structural Engineers*, Vol. 30, Issue 5, 1308-1318.
- Kaewkulchai, G., Williamson, E. B., 2004. Beam element formulation and solution procedure for dynamic progressive collapse analysis. *Journal of Computers & Structures*, Vol. 82, Issues 7-8, pp. 639-651.
- Kent, D., and Park, R. 1971. Flexural members with confined concrete. *Journal of the Structural Division, American Society of Civil Engineers*, Vol. 97, Issue 7, 1969-1990.
- Kim, J., and Park, J. 2008. Design of steel moment frames considering progressive collapse. *Steel and Composite Structures*, Vol. 8, Issue 1, 85-98.
- Kim, T., Kim, J., and Park, J. 2008. Investigation of progressive collapse-resisting capability of steel moment frames using push-down analysis. *Journal of Performance of Constructed Facilities*, Vol. 23, Issue 5, 327-335.
- Lim, J. 2004. Progressive collapse analyses of steel framed moment resisting structures. Ph.D. thesis, Collage of Engineering, The Pennsylvania State University, PA.
- Lin, L., Naumoski, N., Saatcioglu, M., and Foo, S. 2011. Assessment of the vulnerability of buildings to progressive collapse due to blast loads. *Proceedings of the 2011 Canadian Society for Civil Engineering General Conference, Ottawa, Ont.*, pp. 10.
- Liu, J., Tian, Y., Orton, S. L., and Said, A. M. 2015. Resistance of flat-plate buildings against progressive collapse. I: Modeling of slab-column connections. *Journal of Structural Engineering*, 04015053.

Livingston, E., Sasani, M., Bazan, M., and Sagioglu, S. 2015. Progressive collapse resistance of RC beams. *Journal of Engineering Structures*, Vol. 95, 61-70.

Mainstone, R. J. 1973. The hazard of internal blast in buildings. *Building Research Establishment Current Paper*, Report No. 81, Building Research Station, Garston, Watford.

Mirvalad, S. J. 2013. Robustness and retrofit strategies for seismically-designed multistory steel frame buildings prone to progressive collapse. M.A.Sc. thesis, Department of Building, Civil and Environmental Engineering, Concordia University, Montreal, QC.

Mlakar, P. F. 2003. The Pentagon building performance report. American Society of Civil Engineers, ISBN 0-7844-0638-3, Reston, VA.

Mlakar, P., Dusenberry, D., Harris, J., Haynes, G., Phan, L., and Sozen, M. 2003. Findings and recommendations from pentagon crash. Third Forensic Engineering Congress. American Society of Civil Engineers, San Diego, CA.

Monsted, J. M. 1979. Buildings susceptible to progressive collapse. *International Journal for Housing Science and Its Application*, Vol. 3, No.1, 55-67.

Murtha-Smith, E. 1988. Alternate path analysis of space trusses for progressive collapse. *Journal of Structural Engineering*, Vol. 114, Issue 9, 1978-1999.

National Academy of Science. 1995. Protecting buildings from bomb damage. National Academy Press, Washington, D.C.

NBCC. 2010. National Building Code of Canada 2010. Institute for Research in Construction, National Research Council of Canada, Ottawa, Ont.

NISTIR 7396. 2007. Best practices for reducing the potential for progressive collapse in buildings. National Institute of Standards and Technology, U.S. Department of Commerce.

Orton, S. L. 2007. Development of a CFRP system to provide continuity in existing reinforced concrete buildings vulnerable to progressive collapse. Ph.D. thesis, Faculty of the Graduate school, The University of Texas at Austin, Austin, TX.

- Pearson, C., and Delatte, N. 2005. Ronan Point apartment tower collapse and its effect on building codes. *Journal of Performance of Constructed Facilities*, Vol. 19, Issue 2, 172-177
- Pekau, O. A. 1982. Structural integrity of precast panel shear walls. *Canadian Journal of Civil Engineering*, Vol.9, No.1, 13-24.
- Popoff, A. J. 1975. Design against progressive collapse. *PCI Journal*, Vol. 20, Issue 2, 44-57.
- Pretlove, A. J., Ramsden, M., Atkins, A. G., 1991. Dynamic effects in progressive failure of structures. *International Journal of Impact Engineering*, Vol. 11, Issue 4, 539-546.
- Qian, K., and Li, B. 2013. Performance of three-dimensional reinforced concrete beam-column substructures under loss of a corner column scenario, Vol. 139, Issue 4, 584-594.
- Sasani, M., and Kropelnicki, J. 2008. Progressive collapse analysis of an RC structure. *The Structural Design of Tall and Special Buildings*, Vol. 17, Issue 4, 757-771.
- Shankar, R. 2004. Progressive collapse basics. American Institute of Steel Construction Inc., (www.aisc.org).
- Sinaei, H., Shariati, M., Abna, A., Aghaei, M., and Shariati, A. 2012. Evaluation of reinforced concrete beam behaviour using finite element analysis by ABAQUS. *Scientific Research and Essays*, Vol. 7, Issue 21, 2002-2009.
- Smilowitz, R., Hapij, A., and Smilow, J. 2002. Bankers Trust Building. World Trade Center Building Performance Study, Federal Emergency Management Agency, New York.
- Tran, C., and Li, B. 2015. Experimental studies on the backbone curves of reinforced concrete column with light transverse reinforcement. *Journal of Performance of Constructed Facilities*, Vol. 29, Issue 5, 04014126(1)-(11).
- U.S. Department of Defense. 2013. Unified facilities criteria (UFC) - Design of buildings to resist progressive collapse, UFC 4-023-03. U.S. Department of Defense, Washington, D.C.

Valipour, H. R., and Foster, S. J. 2010. Finite element modelling of reinforced concrete framed structures including catenary action. *Computers and Structures*, Vol.88, Issues 9-10, 529-538.

Webster, F. A. 1980. Reliability of multistory slab structures against progressive collapse during construction. *Journal of The American Concrete Institute*, Vol. 77, Issue. 6, 449-457.

Xiao, Y., Kunnath, S., Li, F. W., Zhao, Y. B., Lew, H. S., and Bao, Y. 2015. Collapse test of three-story half-scale reinforced concrete frame building. *ACI Structural Journal*, Vol. 112, Issue 4, 429-438.

Yagob, O., Galal, K., and Naumoski, N. 2009. Progressive collapse of reinforced concrete structures. *Journal of Structural Engineering and Mechanics*, Vol. 32, Issue 6, 771-786.

Yu, J., and Tan, K.H. 2013. Experimental and numerical investigation on progressive collapse resistance of reinforced concrete beam column sub-assemblages. *Engineering Structures*, Vol. 55, 90-106.